Rain or Snow: Hydrologic Processes, Observations, Prediction, and Research Needs

Adrian A. Harpold*, University of Nevada, Reno, aharpold@cabnr.unr.edu
Michael Kaplan, Desert Research Institute, michael.kaplan@dri.edu
P. Zion Klos, University of Idaho, zion.klos@gmail.com
Timothy Link, University of Idaho, tlink@uidaho.edu
James P. McNamara, Boise State University, jmcnamar@boisestate.edu
Seshadri Rajagopal, Desert Research Institute, Seshadri.Rajagopal@dri.edu
Rina Schumer, Desert Research Institute, rina@dri.edu
Caitriana M. Steele, New Mexico State University, caiti@nmsu.edu

*Corresponding author

Abstract

The phase of precipitation when it reaches the ground is a first-order driver of hydrologic processes in a watershed. The presence of snow, rain, or mixed phase precipitation affects the initial and boundary conditions that drive hydrological models. Despite their foundational importance to terrestrial hydrology, typical phase prediction methods (PPM) specify phase based on near-surface air temperature only. Our review conveys the diversity of tools available for PPM in hydrological modeling and the advancements needed to improve predictions in complex terrain with large spatiotemporal variations in precipitation phase. Initially, we review the processes and physics that control precipitation phase as relevant to hydrologists, focusing on the importance of processes occurring aloft. There is a wide range of options for field observations of precipitation phase, but there is a lack of a robust observation networks in complex terrain. New remote sensing observations have potential to increase PPM fidelity, but generally require assumptions typical of other PPM and field validation before they are operational. We review common PPM and find that accuracy is generally increased at finer measurement intervals and by including humidity information. One important tool for PPM development is atmospheric modeling, which includes microphysical schemes that have not been effectively linked to hydrological models or validated against near-surface precipitation phase observations. The review concludes by describing key research gaps and recommendations to improve PPM, including better incorporation of atmospheric information, improved validation datasets, and regional-scale gridded data products. Two key points emerge from this synthesis for the hydrologic community: 1) current PPM are too simple to capture important processes and are not well-validated for most locations, 2) lack of sophisticated PPM increases the uncertainty in estimation of hydrological sensitivity to changes in precipitation phase at local to regional scales. The advancement of PPM is a critical research frontier in hydrology that requires scientific cooperation between hydrological and atmospheric modelers and field scientists.

Keywords: precipitation phase, snow, rain, hydrological modeling

1. Introduction and Motivation

As climate warms, a major hydrologic shift in precipitation phase from snow to rain is expected to occur across temperate regions that are reliant on mountain snowpacks for water resource provisioning (Bales et al., 2006; Barnett et al., 2005). Continued changes in precipitation phase

are expected to alter snowpack dynamics and both streamflow timing and amounts (Cayan et al., 2001; Fritze et al., 2011; Luce and Holden, 2009; Klos et al., 2014; Berghuijs et al., 2014; Jepsen et al., 2016), increase rain-on snow flooding (McCabe et al., 2007), and challenge our ability to make accurate water supply forecasts (Milly et al., 2008). Accurate estimations of precipitation inputs are required for effective hydrological modeling in both applied and research settings. Snow storage delays the transfer of precipitation to surface runoff, infiltration, and generation of streamflows (Figure 1), affecting the timing and magnitude of peak flows (Wang et al., 2016), hydrograph recession (Yarnell et al., 2010) and the magnitude and duration of summer baseflow (Safeeq et al., 2014; Godsey et al., 2014). Moreover, the altered timing and rate of snow versus rain inputs can modify the partitioning of water to evapotranspiration versus runoff (Wang et al., 2013). Misrepresentation of precipitation phase within hydrologic models thus propagates into spring snowmelt dynamics (Harder and Pomeroy, 2013; Mizukami et al., 2013; White et al., 2002; Wen et al., 2013) and streamflow estimates used in water resource forecasting (Figure 1). The persistence of streamflow error is particularly problematic for hydrological models that are calibrated on observed streamflows because this error can be compensated for by altering parameters that control other states and fluxes in the model (Minder, 2010; Shamir and Georgakakos, 2006; Kirchner, 2006). Expected changes in precipitation phase from climate warming presents a new set of challenges for effective hydrological modeling (Figure 1). A simple yet essential issue for nearly all runoff generation questions is this: Is precipitation falling as rain, snow, or a mix of both phases?

Despite advances in terrestrial process-representation within hydrological models in the past several decades (Fatichi et al., 2016), most state-of-the-art models rely on simple empirical algorithms to predict precipitation phase. For example, nearly all operational models used by the National Weather Service River Forecast Centers in the United States use some type of temperature-based precipitation phase partitioning method (PPM) (Pagano et al., 2014). These are often single or double temperature threshold models that do not consider other conditions important to the hydrometeor's energy balance. Although forcing datasets for hydrological models are rapidly being developed for a suite of meteorological variables, to date no gridded precipitation phase product has been developed over regional to global scales. Widespread advances in both simulation of terrestrial hydrological processes and computational capabilities

may have limited improvements on water resources forecasts without commensurate advances in PPM.

Recent advances in PPM incorporate effects of humidity (Harder and Pomeroy, 2013; Marks et al., 2013), atmospheric temperature profiles (Froidurot et al., 2014), and remote sensing of phase in the atmosphere (Minder, 2010; Lundquist et al., 2008). A challenge to improving and selecting PPM is the lack of validation data. In particular, reliable ground-based observations of phase are sparse, collected at the point scale over limited areas, and are typically limited to research rather than operational applications (Marks et al., 2013). The lack of observations is particularly problematic in mountain regions where snow-rain transitions are widespread and critical for regional water resource evaluations (Klos et al., 2014). For example, direct visual observations have been widely used (Froidurot et al., 2014; Knowles et al., 2006; U.S. Army Corps of Engineers, 1956), but are decreasing in number in favor of automated measurement systems. Automated systems use indirect methods to accurately estimate precipitation phase from hydrometeor characteristics (i.e. disdrometers), as well as coupled measurements that infer precipitation phase based on multiple lines of evidence (e.g. co-located snow depth and precipitation). Remote sensing is another indirect method that typically uses radar returns from ground and space-borne platforms to infer hydrometeor temperature and phase. A comprehensive description of the advantages and disadvantages of current measurement strategies, and their correspondence with conventional PPM, is needed to determine critical knowledge gaps and research opportunities.

New efforts are needed to advance PPM to better inform hydrological models by integrating new observations, expanding the current observation networks, and testing techniques over regional variations in hydroclimatology. While calls to integrate atmospheric information are an important avenue for advancement (Feiccabrino et al., 2013), hydrological models ultimately require accurate and validated phase determination at the land surface. Moreover, any advancement that relies on integrating new information or developing a new PPM technique will require validation and training using ground-based observations. To make tangible hydrological modeling advancements, new techniques and datasets must be integrated with current modeling tools. The first step towards improved hydrological modeling in areas with mixed precipitation

phase is educating the scientific community about current techniques and limitations that convey the areas where research is most needed.

Our review paper is motivated by a lack of a comprehensive description of the state-of-the-art PPM and observation tools. Therefore, we describe the current state of the science in a way that clarifies the correspondence between techniques and observations, and highlights strengths and weaknesses in the current scientific understanding. Specifically, subsequent sections will review: 1) the processes and physics that control precipitation phase as relevant to field hydrologists, 2) current available options for observing precipitation phase and related measurements common in remote field settings, 3) existing methods for predicting and modeling precipitation phase, and 4) research gaps that exist regarding precipitation phase estimation. The overall objective is to convey a clear understanding of the diversity of tools available for PPM in hydrological modeling and the advancements needed to improve predictions in complex terrain characterized by large spatiotemporal variations in precipitation phase.

2. Processes and Physics Controlling Precipitation Phase

Precipitation formed in the atmosphere is typically a solid in the mid-latitudes and its phase at the land surface is determined by whether it melts during its fall (Stewart et al., 2015). Most hydrologic models do not simulate atmospheric processes and specify precipitation phase based on surface conditions alone (see Section 4.1), ignoring phase transformations in the atmosphere.

Several important properties that influence phase changes in the atmosphere are not included in hydrological models (Feiccabrino et al., 2012), such as temperature and precipitation characteristics (Theriault and Stewart, 2010), stability of the atmosphere (Theriault and Stewart, 2007), position of the 0 °C isotherm (Minder, 2010; Theriault and Stewart, 2010), interaction between hydrometeors (Stewart, 1992), and the atmospheric humidity profile (Harder and Pomeroy, 2013). The vertical temperature and humidity (represented by the mixing ratio) profile through which the hydrometeor falls typically consists of three layers, a top layer that is frozen ($T < 0$ °C) in winter in temperate areas (Stewart, 1992), a mixed layer where T can exceed 0 °C, and a surface layer that can be above or below 0 °C (Figure 2). The phase of precipitation at the surface partly depends on the phase reaching the top of the surface layer, which is defined as the

critical height. The temperature profile and depth of the surface layer control the precipitation phase reaching the ground surface. For example, in Figure 2a, if rain reaches the critical height, it may reach the surface as rain or ice pellets depending on small differences in temperature in the surface layer (Theriault and Stewart, 2010). Similarly, in Figure 2b, if snow reaches the critical height, it may reach the surface as snow if the temperature in the surface layer is below freezing. However, in Figure 2c, when the surface layer temperatures are close to freezing and the mixing ratios are neither close to saturation nor very dry, the phase at the surface is not easily determined by the surface conditions alone.

In addition to strong dependence on the vertical temperature and humidity profiles, precipitation phase is also a function of fall rate and hydrometeor size because they affect energy exchange with the atmosphere (Theriault et al., 2010). Precipitation rate influences the precipitation phase; for example, a precipitation rate of 10 mm h^{-1} reduces the amount of freezing rain by a factor of three over a precipitation rate of 1 mm h^{-1} (Theriault and Stewart, 2010) because there is less time for turbulent heat exchange with the hydrometeor. A solid hydrometeor that originates in the top layer and falls through the mixed layer can reach the surface layer as wet snow, sleet, or rain. This phase transition in the mixed layer is primarily a function of latent heat exchange driven by vapor pressure gradients and sensible heat exchange driven by temperature gradients. Temperature generally increases from the mixed layer to the surface layer causing sensible heat inputs to the hydrometeor. If these gains in sensible heat are combined with minimal latent heat losses resulting from low vapor pressure deficits, it is likely that the hydrometeor will reach the surface layer as rain (Figure 2). However, vapor pressure in the mixed layer is often below saturation leading to latent energy losses and cooling of the hydrometeor coupled with diabatic cooling of the local atmosphere, which can produce snow or other forms of frozen precipitation at the surface even when temperatures are above 0 °C. Likewise, surface energetics affect local atmospheric conditions and dynamics, especially in complex terrain. For example, melting of the snowpack can cause diabatic cooling of the local atmosphere and affect the phase of precipitation, especially when air temperatures are very close to 0 °C (Theriault et al., 2012). Many conditions lead to a combination of latent heat losses and sensible heat gains by hydrometeors (Figure 2). Under these conditions it can be difficult to predict the phase of

precipitation without sufficient information about humidity and temperature profiles, turbulence, hydrometeor size, and precipitation intensity.

Stability of the atmosphere can also influence precipitation phase. Stability is a function of the vertical temperature structure which can be altered by vertical air movement and hence influence precipitation phase (Theriault and Stewart, 2007). Vertical air velocity changes the temperature structure by adiabatic warming or cooling due to pressure changes of descending and ascending air parcels, respectively. These changes in temperature can generate under-saturated or supersaturated conditions in the atmosphere that can also alter the precipitation phase. Even a very weak vertical air velocity (< 10 cm/s) significantly influences the phase and amount of precipitation formed in the atmosphere (Theriault and Stewart, 2007). The rain-snow line predicted by atmospheric models is very sensitive to these microphysics (Minder, 2010) and validating the microphysics across locations with complex physiography is challenging. Incorporation and validation of atmospheric microphysics is rarely achieved in hydrological applications (Feiccabrino et al., 2015).

3. Current Tools for Observing Precipitation Phase

3.1 In situ observations

In situ observations refer to methods wherein a person or instrument onsite records precipitation phase. We identify 3 classes of approaches that are used to observe precipitation phase including 1) direct observations, 2) coupled observations, and 3) proxy observations.

Direct observations simply involve a person on-site noting the phase of falling precipitation. Such data form the basis of many of the predictive methods that are widely used (Dai, 2008; Ding et al., 2014; U.S. Army Corps of Engineers, 1956). Direct observations are useful for "manned" stations such as those operated by the U.S. National Weather Service. Few research stations however, have this benefit, particularly in many remote regions and in complex terrain. Direct observations are also limited in their temporal resolution and are typically reported only once per day, with some exceptions (Froidurot et al., 2014). Citizen scientist networks have historically provided valuable data to supplement primary instrumented observation networks. The National Weather Service Cooperative Observer Program (http://www.nws.noaa.gov/om/coop/what-is-coop.html, accessed 10/12/2016) is comprised of a

network of volunteers recording daily observations of temperature and precipitation, including phase. The NOAA National Severe Storms Laboratory used citizen scientist observations of rain and snow occurrence to evaluate the performance of the Multi-Radar Multi-Sensor (MRMS) system in the meteorological Phenomena Identification Near the Ground (mPING) project (Chen et al., 2015). The mPING project has recently been expanded to allow citizen scientists worldwide to easily report precipitation phase and characteristics using GPS-enabled smartphone applications (http://mping.nssl.noaa.gov, accessed 12/4/2016). The Colorado Climate Center initiated the Community Collaborative Rain, Hail and Snow Network (CoCoRaHS) which supplies volunteers with low cost instrumentation to observe precipitation characteristics, including phase, and enables observations to be reported on the project website (http://www.cocorahs.org/, accessed 10/12/2016). Although highly valuable, some limitations of this system include the imperfect ability of observers to identify mixed phase events and the temporal extent of storms, as well as the lack of observations in both remote areas and during low light conditions.

Coupled observations link synchronous measurements of precipitation with secondary observations to indicate phase. Secondary observations can include photographs of surrounding terrain, snow depth measurements, and/or measurements of ancillary meteorological variables. Photographs of vertical scales emplaced in the snow have been used to estimate snow accumulation depth, which can then be coupled with precipitation mass to determine density and phase (Berris and Harr, 1987; Floyd and Weiler, 2008; Garvelmann et al., 2013; Hedrick and Marshall, 2014; Parajka et al., 2012). Mixed phase events however, are difficult to quantify using coupled depth- and photographic-based techniques (Floyd and Weiler, 2008). Acoustic distance sensors, which are now commonly used to monitor the accumulation of snow (e.g. Boe, 2013), have similar drawbacks in mixed phase events, but have been effectively applied to discriminate between snow and rain (Rajagopal and Harpold, 2016). Meteorological information such as temperature and relative humidity can be used to compute the phase of precipitation measured by bucket-type gauges. Unfortunately, this approach generally requires incorporating assumptions about the meteorological conditions that determine phase (see section 4.1). Harder and Pomeroy (2013) used a comprehensive approach to determine the phase of precipitation. Every 15 minutes during their study period phase was determined by evaluating weighing bucket mass, tipping

bucket depth, albedo, snow depth, and air temperature. Similarly, Marks et al. (2013) used a scheme based on co-located precipitation and snow depth to discriminate phase. A more involved expert decision making approach by L'hôte et al. (2005) was based on six recorded meteorological parameters: precipitation intensity, albedo of the ground, air temperature, ground surface temperature, reflected long-wave radiation, and soil heat flux. The intent of most of these coupled observations was to develop datasets to evaluate PPM. However, if observation systems such as these were sufficiently simple, they could have the potential to be applied operationally across larger meteorological monitoring networks encompassing complex terrain where snow comprises a large component of annual precipitation (Rajagopal and Harpold, 2016).

Proxy observations measure geophysical properties of precipitation to infer phase. The hot plate precipitation gauge introduced by Rasmussen et al. (2012), for example, uses a thin heated disk to accumulate precipitation and then measures the amount of energy required to melt snow or evaporate liquid water. This technique however, requires a secondary measurement of air temperature to determine if the energy is used to melt snow or only evaporate rain. Disdrometers measure the size and velocity of hydrometeors. Although the most common application of disdrometer data is to determine the drop size distribution (DSD) and other properties of rain, the phase of hydrometeors can be inferred by relating velocity and size to density. Some disdrometer technologies, which can be grouped into impact, imaging, and scattering approaches (Loffler-Mang et al., 1999), are better suited for describing snow than others. Impact disdrometers, first introduced by Joss and Waldvogel (1967), use an electromechanical sensor to convert the momentum of a hydrometeor into an electric pulse. The amplitude of the pulse is a function of drop diameter. Impact disdrometers have not been commonly used to measure solid precipitation due to the different functional relationships between drop size and momentum for solid and liquid precipitation. Imaging disdrometers use basic photographic principles to acquire images of the distribution of particles (Borrmann and Jaenicke, 1993; Knollenberg, 1970). The 2D Video Disdrometer (2DVD) described by Kruger and Krajewski (2002) records the shadows cast by hydrometeors onto photodetectors as they pass through two sheets of light. The shape of the shadows enables computation of particle size, and shadows are tracked through both light sheets to determine velocity. Although initially designed to describe liquid precipitation, recent work has shown that the 2DVD can be used to classify snowfall according to microphysical properties

of single hydrometeors (Bernauer et al., 2016). The 2DVD has been used to classify known rain and snow events, but little work has been performed to distinguish between liquid and solid precipitation. Scattering or optical disdrometers, measure the extinction of light passing between a source and a sensor (Hauser et al., 1984; Loffler-Mang et al., 1999). Like the other types, optical disdrometers were originally designed for rain, but have been periodically applied to snow (Battaglia et al., 2010; Lempio et al., 2007). In a comparison study by Caracciolo et al. (2006), the PARSIVEL optical disdrometer, originally described by Loffler-Mang et al. (1999) did not perform well against a 2DVD because of problems related to the detection of slow fall velocities for snow. It may be possible to use optical disdrometers to distinguish between rain, sleet, and snow based on the existence of distinct shapes of the size spectra for each precipitation type. More research on the relationship between air temperature and the size spectra produced by the optical disdrometer is needed (Lempio et al., 2007). In summary, disdrometers of various types are valuable tools for describing the properties of rain and snow, but require further testing and development to distinguish between rain and snow, as well as mixed phase events.

3.2 Ground-based remote sensing observations

Ground-based remote sensing observations have been available for several decades to detect precipitation phase using radar. Until recently, most ground-based radar stations were operated as conventional Doppler systems that transmit and receive radio waves with single horizontal polarization. Developments in dual polarization ground radar such as those that function as part of the U.S. National Weather Service NEXRAD network (NOAA, 2016), have resulted in systems that transmit radio signals with both horizontal and vertical polarizations. In general, ground-based remote sensing observations, either single or dual-pol, remain underutilized for detecting precipitation phase and are challenging to apply in complex terrain (Table 3).

Ground-based remote sensing of precipitation phase using single-polarized radar systems depends on detecting the radar bright band. Radio waves transmitted by the radar system, are scattered by hydrometeors in the atmosphere, with a certain proportion reflected back towards the radar antenna. The magnitude of the measured reflectivity (Z) is related to the size and the dielectric constant of falling hydrometeors (White et al., 2002). Ice particles aggregate as they descend through the atmosphere and their dielectric constant increases, in turn increasing Z

297 measured by the radar, creating the bright band, a layer of enhanced reflectivity just below the
298 elevation of the melting level (Lundquist et al., 2008). Therefore, bright band elevation can be
299 used as a proxy for the "snow level", the bottom of the melting layer where falling snow
300 transforms to rain (White et al., 2010;White et al., 2002).
301
302 Doppler vertical velocity (DVV) is another variable that can be estimated from single-polarized
303 vertically profiling radar. DVV gives an estimate of the velocity of falling particles; as
304 snowflakes melt and become liquid raindrops, the fall velocity of the hydrometeors increases.
305 When combined with reflectivity profiles, DVV helps reduce false positive detection of the
306 bright band, which may be caused by phenomena other than snow melting to rain (White et al.,
307 2002). First, DVV and Z are combined to detect the elevation of the bottom of the bright band.
308 The algorithm then searches for maximum Z above the bottom of the bright band and determines
309 that to be the bright band elevation (White et al., 2002). However, a test of this algorithm on data
310 from a winter storm over the Sierra Nevada found root mean square errors of 326 to 457 m
311 compared to ground observations when the bright band elevation was assumed to represent the
312 surface transition from snow to rain (Lundquist et al., 2008). Snow levels in mountainous areas
313 however, may also be overestimated by radar profiler estimates if they are unable to resolve
314 spatial variations close to mountain fronts, since snow levels have been noted to persistently drop
315 on windward slopes (Minder and Kingsmill, 2013). Despite the potential errors, the elevation of
316 maximum Z may be a useful proxy for snow level in hydrometeorological applications in
317 mountainous watersheds because maximum Z will always occur below the freezing level
318 (Lundquist et al., 2008; White et al., 2010)
319
320 Few published studies have explored the value of bright band-derived phase data for hydrologic
321 modeling. Maurer and Mass (2006) compared the melting level from vertically pointing radar
322 reflectivity against temperature-based methods to assess whether the radar approach could
323 improve determination of precipitation phase at the ground level. In that study, the altitude of the
324 top of the bright band was detected and applied across the study basin. Frozen precipitation was
325 assumed to be falling in model pixels above the altitude of the melting level and liquid
326 precipitation was assumed to be falling in pixels below the altitude of the melting layer (Maurer
327 and Mass, 2006). Maurer and Mass (2006) found that incorporating radar-detected melting layer

328 altitude improved streamflow simulation results. A similar study that used bright band altitude to
329 classify pixels according to surface precipitation type was not as conclusive; bright band altitude
330 data did not improve hydrologic model simulation results over those based on a temperature
331 threshold (Mizukami et al., 2013). Also, the potential of the method is limited to the availability
332 of vertically pointing radar; in complex, mountainous terrain the ability to estimate melting level
333 becomes increasingly challenging with distance from the radar.
334
335 Dual-polarized radar systems generate more variables than traditional single-polarized systems.
336 These polarimetric variables include differential reflectivity, reflectivity difference, the
337 correlation coefficient, and specific differential phase. Polarimetric variables respond to
338 hydrometeor properties such as shape, size, orientation, phase state, and fall behavior and can be
339 used to assign hydrometeors to specific categories (Chandrasekar et al., 2013; Grazioli et al.,
340 2015), or to improve bright band detection (Giangrande et al., 2008).
341
342 Various hydrometeor classification algorithms have been applied to X-, C-, and S-band
343 wavelengths. Improvements in these algorithms over recent years have seen hydrometeor
344 classification become an operational meteorological product (see Grazioli et al., 2015 for an
345 overview). For example, the U.S. National Severe Storms Laboratory (NSSL) developed a fuzzy-
346 logic hydrometeor classification algorithm for warm-season convective weather (Park et al.,
347 2009) and this algorithm has also been tested for cold-season events (Elmore, 2011). Its skill was
348 tested against surface observations of precipitation type but the algorithm did not perform well in
349 classifying winter precipitation because it could not account for re-freezing of hydrometeors
350 below the melting level (Figure 2, Elmore, 2011). Unlike warm season convective precipitation,
351 the freezing level during a cold-season precipitation event can vary spatially. This phenomenon
352 has prompted the use of polarimetric variables to first detect the melting layer, and then classify
353 hydrometeors (Boodoo et al., 2010; Thompson et al., 2014). Although there has been some
354 success in developing two-stage cold-season hydrometeor classification algorithms, there is little
355 in the published literature that explores the potential contributions of these algorithms for
356 partitioning snow and rain for hydrological modeling.
357

3.3 Space-based remote sensing observations

Spaceborne remote sensing observations typically use passive or active microwave sensors to determine precipitation phase (Table 3). Many of the previous passive microwave systems were challenged by coarse resolutions and difficulties retrieving snowfall over snow-covered areas. More recent active microwave systems are advantageous for detecting phase in terms of accuracy and spatial resolution, but remain largely unverified. Table 3 provides and overview of these space-based remote sensing technologies that are described in more detail below.

Passive microwave radiometers detect microwave radiation emitted by the Earth's surface or atmosphere. Passive microwave remote sensing has the potential for discriminating between rainfall and snowfall because microwave radiation emitted by the Earth's surface propagates through all but the densest precipitating clouds, meaning that radiation at microwave wavelengths directly interacts with hydrometeors within clouds (Olson et al., 1996; Ardanuy, 1989). However, the remote sensing of precipitation in microwave wavelengths and the development of operational algorithms is dominated by research focused on rainfall (Arkin and Ardanuy, 1989); by comparison, snowfall detection and observation has received less attention (Noh et al., 2009; Kim et al., 2008). This is partly explained by examining the physical processes within clouds that attenuate the microwave signal. Raindrops emit low levels of microwave radiation increasing the level of radiance measured by the sensor; in contrast, ice hydrometeors scatter microwave radiation, decreasing the radiance measured by a sensor (Kidd and Huffman, 2011). Land surfaces have a much higher emissivity than water surfaces, meaning that emission-based detection of precipitation is challenging over land because the high microwave emissions mask the emission signal from raindrops (Kidd, 1998; Kidd and Huffman, 2011). Thus, scattering-based techniques using medium to high frequencies are used to detect precipitation over land. Moreover, microwave observations at higher frequencies (> 89 GHz) have been shown to discriminate between liquid and frozen hydrometeors (Wilheit et al., 1982).

Retrieving snowfall over land areas from spaceborne microwave sensors can be even more challenging than for liquid precipitation because existing snow cover increases microwave emission. Depression of the microwave signal caused by scattering from airborne ice particles may be obscured by increased emission of microwave radiation from the snow covered land

surface. Kongoli et al. (2003) demonstrated an operational snowfall detection algorithm that accounts for the problem of existing snow cover. This group used data from the Advanced Microwave Sounding Unit-A (AMSU-A), a 15-channel atmospheric temperature sounder with a single high frequency channel at 89 GHz), and AMSU-B, a 5-channel high frequency microwave humidity sounder. Both sensors were mounted on the NOAA-16 and -17 polar-orbiting satellites. While the algorithm worked well for warmer, opaque atmospheres, it was found to be too noisy for colder, clear atmospheres. Additionally, some snowfall events occur under warmer conditions than those that were the focus of the study (Kongoli et al., 2003). Kongoli et al. (2015) further adapted their methodology for the Advanced Technology Microwave Sounder (ATMS - onboard the polar-orbiting Suomi National Polar-orbiting Partnership satellite) a descendant of the AMSU sounders. The latest algorithm assesses the probability of snowfall using the logistic regression and the principal components of seven high frequency bands at 89 GHz and above. In testing, the Kongoli et al. (2015) algorithm has shown skill in detecting snowfall both at variable rates and when snowfall is lighter and occurs in colder conditions. An alternative algorithm by Noh et al. (2009) used physically-based, radiative transfer modeling in an attempt to improve snowfall retrieval over land. In this case, radiative transfer modeling was used to construct an *a priori* database of observed snowfall profiles and corresponding brightness temperatures. The radiative transfer procedure yields likely brightness temperatures from modeling how ice particles scatter microwave radiation at different wavelengths. A Bayesian retrieval algorithm is then used to estimate snowfall over land by comparing measured and modeled brightness temperatures (Noh et al., 2009). The algorithm was tested during the early and late winter for large snowfall events (e.g. 60 cm depth in 12 hours). Late winter retrievals indicated that the algorithm overestimated snowfall over surfaces with significant snow accumulation.

While results have been promising, the spatial resolution at which ATMS and other passive microwave data are acquired is very coarse (15.8 to 74.8 km at nadir), making passive microwave approaches more applicable for regional to continental scales. Temporal resolution of the data acquisition is another challenge. AMSU instruments are mounted on 8 satellites; the related ATMS is mounted on a single satellite and planned for two additional satellites. However, the satellites are polar-orbiting, not geostationary, so it is probable that a precipitation event could occur outside the field of view of one of the instruments.

Spaceborne active microwave or radar sensors measure the backscattered signal from pulses of microwave energy emitted by the sensor itself. Much like the ground based radar systems, the propagated microwave signal interacts with liquid and solid particles in the atmosphere and the degree to which the measured return signal is attenuated provides information on the atmospheric constituents. The advantage offered by spaceborne radar sensors over passive microwave is the capability to acquire more detailed sampling of the vertical profile of the atmosphere (Kulie and Bennartz, 2009). The first spaceborne radar capable of observing snowfall is the Cloud Profiling Radar (CPR) onboard CloudSat (2006 – present). The CPR operates at 94 GHz with an along-track (or vertical) resolution of ~1.5 km. Retrieval of dry snowfall rate from CPR measurements of reflectivity have been shown to correspond with estimates of snowfall from ground-based radars at elevations of 2.6 and 3.6 km above mean sea level (Matrosov et al., 2008). Estimates at lower elevations, especially those in the lowest 1 km, are contaminated by ground clutter. Alternative approaches, combining CPR data with ancillary data have been formulated to account for this challenge (Kulie and Bennartz, 2009; Liu, 2008). Known relationships between CPR reflectivity data and the scattering properties of non-spherical ice crystals are used to derive snowfall at a given elevation above mean sea level; below this elevation a temperature threshold derived from surface data is used to discriminate between rain and snow events. Liu (2008) used 2 °C as the snow/rain threshold, whereas Kulie and Bennartz (2009) used 0 °C as the snow/rain threshold. Temperature thresholds have been the subject of much research and debate for discriminating precipitation phase, as is further discussed in section 4.1.

CloudSat is part of the A-train or afternoon constellation of satellites, which includes Aqua, with the Moderate Resolution Imaging Spectrometer (MODIS) and the Cloud–Aerosol Lidar and Infrared Pathfinder Satellite Observations (CALIPSO) spacecraft with cloud-profiling Lidar. The sensors onboard A-train satellites provided the unique combination of data to create an operational snow retrieval product. The CPR Level 2 snow profile product (2C-SNOW-PROFILE) uses vertical profile data from the CPR, input from MODIS and the cloud profiling radar, as well as weather forecast data to estimate near surface snowfall (Kulie et al., 2016; Wood et al., 2013). The performance of 2C-SNOW-PROFILE was tested by Cao et al. (2014).

This group found the product worked well in detecting light snow but performed less satisfactorily under conditions of moderate to heavy snow because of the non-stationary effects of attenuation on the returned radar signal.

The launch of the Global Precipitation Mission (GPM) core observatory in February 2014 holds promise for the future deployment of operational snow detection products. Building on the success of the Tropical Rainfall Monitoring Mission (TRMM), the GPM core observatory sensors include the Dual-frequency Precipitation Radar (DPR) and GPM Microwave Imager (GMI). The GMI has two millimeter wave channels (166 and 183 GHz) that are specifically designed to detect and retrieve light rain and snow precipitation. These are more advanced than the sensors onboard the TRMM spacecraft and permit better quantification of the physical properties of precipitating particles, particularly over land at middle to high latitudes (Hou et al., 2014). Algorithms for the GPM mission are still under development, and are partly being driven by data collected during the GPM Cold Season Experiment (GCPEx) (Skofronick-Jackson et al., 2015). Using airborne sensors to simulate GPM and DPR measurements, one of the questions that the GCPEx hoped to address concerned the potential capability of data from the DPR and GMI to discriminate falling snow from rain or clear air (Skofronick-Jackson et al., 2015). The initial results reported by the GCPEx study echo some of the challenges recognized for ground-based single polarized radar detection of snowfall. The relationship between radar reflectivity and snowfall is not unique. For the GPM mission, it will be necessary to include more variables from dual frequency radar measurements, multiple frequency passive microwave measurements, or a combination of radar and passive microwave measurements (Skofronick-Jackson et al., 2015).

4. Current Tools for Predicting Precipitation Phase

4.1 Prediction Techniques from Ground-Based Observations

Discriminating between solid and liquid precipitation is often based on a near-surface air temperature threshold (Martinec and Rango, 1986; U.S. Army Corps of Engineers, 1956; L'hôte et al., 2005). Four prediction methods have been developed that use near-surface air temperature for discriminating precipitation phase: 1) static threshold, 2) linear transition, 3) minimum and maximum temperature, and 4) sigmoidal curve (Table 1). A static temperature threshold applies

a single temperature value, such as mean daily temperature, where all of the precipitation above the threshold is rain, and all below the threshold is snow. Typically this threshold temperature is near 0 °C (Lynch-Stieglitz, 1994; Motoyama, 1990), but was shown to be highly variable across both space and time (Kienzle, 2008; Motoyama, 1990; Braun, 1984; Ye et al., 2013). For example, Rajagopal and Harpold (2016) optimized a single temperature threshold at Snow Telemetry (SNOTEL) sites across the western U.S. to show regional variability from -4 to 3 °C (Figure 3). A second discrimination technique is to linearly scale the proportion of snow and rain between a temperature for all rain (T_{rain}) and a temperature for all snow (T_{snow}) (Pipes and Quick, 1977; McCabe and Wolock, 2010; Tarboton et al., 1995). Linear threshold models have been parameterized slightly differently across studies, e.g.: T_{snow} =-1.0 °C, T_{rain} = 3.0 °C (McCabe and Wolock, 2010), T_{snow} =-1.1 °C and T_{rain} =3.3 °C (Tarboton et al., 1995), and T_{snow} =0 °C and T_{rain} =5 °C (McCabe and Wolock, 1999b). A third technique specifies a threshold temperature based on daily minimum and maximum temperatures to classify rain and snow, respectively, with a threshold temperature between the daily minimum and maximum producing a proportion of rain and snow (Leavesley et al., 1996). This technique can have a time-varying temperature threshold or include a T_{rain} that is independent of daily maximum temperature. A fourth technique applies a sigmoidal relationship between mean daily (or sub daily) temperature and the proportion or probability of snow versus rain. For example, one method derived for southern Alberta, Canada employs a curvilinear relationship defined by two variables, a mean daily temperature threshold where 50% of precipitation is snow, and a temperature range where mixed-phase precipitation can occur (Kienzle, 2008). Another sigmoidal-based empirical model identified a hyperbolic tangent function defined by four parameters to estimate the conditional snow (or rain) frequency based on a global analysis of precipitation phase observations from over 15,000 land-based stations (Dai, 2008). Selection of temperature-based techniques is typically based on available data, with a limited number of studies quantifying their relative accuracy for hydrological applications (Harder and Pomeroy, 2014).

Several studies have compared the accuracy of temperature-based PPM to one another and/or against an independent validation of precipitation phase. Sevruk (1984) found that only about 68% of the variability in monthly observed snow proportion in Switzerland could be explained by threshold temperature based methods near 0 °C. An analysis of data from fifteen stations in

513 southern Alberta, Canada with an average of >30 years of direct observations noted over-
514 estimations in the mean annual snowfall for static threshold (8.1%), linear transition (8.2%),
515 minimum and maximum (9.6%), and sigmoidal transition (7.1%) based methods (Kienzle, 2008).
516 An evaluation of PPM at three sites in the Canadian Rockies by Harder and Pomeroy (2013)
517 found the largest percent error to occur using a static threshold (11% to 18%), followed by linear
518 relationships (-8% to 11%), followed by sigmoidal relationships (-3 to 11%). Another study
519 using 824 stations in China with >30 years of direct observations found accuracies of 51.4%
520 using a static 2.2 °C threshold and 35.7% to 47.4% using linear temperature-based thresholds
521 (Ding et al., 2014). Lastly, for multiple sites across the rain-snow transition in southwestern
522 Idaho, static temperature thresholds produced the lowest proportion (68%) whereas a linear-
523 based model produced the highest proportion (75%) of snow, respectively (Marks et al., 2013).
524 These accuracy assessments generally demonstrated that static threshold methods produced the
525 greatest errors, whereas sigmoidal relationships produced the smallest errors, although variations
526 to this general rule existed across sites.
527
528 Near surface humidity also influences precipitation phase (see Section 2). Three humidity-
529 dependent precipitation phase identification methods are found in the literature: 1) dewpoint
530 temperature (T_d), 2) wet bulb temperature (T_w), and 3) psychometric energy balance. The
531 dewpoint temperature is the temperature at which an air parcel with a fixed pressure and
532 moisture content would be saturated. In one approach to account for measurement and
533 instrument calibration uncertainties of ±0.25 °C each, T_d and T_w below -0.5 °C was assumed to
534 be all snow and above +0.5 °C all rain, with a linear relationship between the two being a
535 proportional mix of snow and rain (Marks et al., 2013). T_d of 0.0 °C performed consistently
536 better than T_a in one study by Marks et al. (2001) while a T_d of 0.1°C for multiple stations in
537 Sweden was less accurate than a T_a of 1.0 °C (Feiccabrino et al., 2013). The wet or ice bulb
538 temperature (T_w) is the temperature at which an air parcel would become saturated by
539 evaporative cooling in the absence of other sources of sensible heat, and is the lowest
540 temperature that falling precipitation can reach. Few studies have investigated the feasibility of
541 T_w for precipitation phase prediction (Olsen, 2003; Ding et al., 2014; Marks et al., 2013). T_w
542 significantly improved prediction of precipitation phase over T_a at 15-minute time steps, but only
543 marginally improved predictions at daily time steps (Marks et al., 2013). Ding et al. (2014)

developed a sigmoidal phase probability curve based on T_w and elevation that outperformed T_a threshold-based methods across a network of sites in China. Conceptually, the hydrometeor temperature (T_i) is similar to T_w but is calculated using the latent heat and vapor density gradient. Use of computed T_i values significantly improved precipitation phase estimates over T_a, particularly as time scales approached one day (Harder and Pomeroy, 2013).

There has been limited validation of humidity-based precipitation phase prediction techniques against ground-truth observations. Ding et al. (2014) showed that a method based on T_w and elevation increased accuracy by 4.8% to 8.9% over several temperature-based methods. Their method was more accurate than a simpler T_w based method by Yamazaki (2001). Feiccabrino et al. (2013) showed that T_d misclassified 3.0% of snow and rain (excluding mixed phase precipitation), whereas T_a only misclassified 2.4%. Ye et al. (2013) found T_d less sensitive to phase discrimination under diverse environmental conditions and seasons than T_a. Froidurot et al. (2014) evaluated several techniques with a critical success index (CSI) at sites across Switzerland to show the highest CSI values were associated with variables that included T_w or relative humidity (CSI=84%-85%) compared to T_a (CSI=78%). Marks et al. (2013) evaluated the time at which precipitation transitioned from snow to rain against field observations across a range of elevations and found that T_d most closely predicted the timing of phase change, whereas both T_a and T_w estimated earlier phase changes than observed. Harder and Pomeroy (2013) compared T_i with field observations and found that error was <10% when T_i was allowed to vary with each daily time-step and >10% when T_i was fixed at 0 °C. The T_i accuracy increased appreciably (i.e. 5%-10% improvement) when the temporal resolution was decreased from daily to hourly or 15-minute time steps. The validation studies consistently showed improvements in accuracy by including humidity over PPM based only on temperature.

Hydrological models employ a variety of techniques for phase prediction using ground-based observations (Table 2). All discrete hydrological models (i.e. not coupled to an atmospheric model) investigated used temperature based thresholds that did not consider the near-surface humidity. Moreover, most models use a single static temperature threshold that typically produces lower accuracy than multiple temperature methods. It should be noted that many of these hydrological models lump by elevation zone, which improves estimates of the snow to rain

transition elevation and phase prediction accuracy in complex terrain compared to models without elevation zones. Hydrological models that are coupled to atmospheric models were more able to consider important controls on precipitation phase, such as humidity and atmospheric profiles. This compendium of model PPM highlights the current shortcomings in phase prediction in conventional discrete hydrological models.

4.2 Prediction Techniques Incorporating Atmospheric Information

While many hydrologic models have their own formulations for determining precipitation phase at the ground, it is also possible to initialize hydrologic models with precipitation phase fraction, intensity, and volume from numerical weather simulation model output. Here we discuss the limitations of precipitation phase simulation inherent to the Weather Research and Forecasting (WRF) model (Kaplan et al., 2012; Skamarock et al., 2008) and other atmospheric simulation models. The finest scale spatial resolution employed in atmospheric simulation models is ~1 km and these models generate data at hourly or finer temporal resolutions. Regional climate models (RCM) and global climate models (GCM) are typically coarser than local mesoscale models. The physical processes driving both the removal of moisture from the air and the precipitation phase (Section 2) occur at much finer spatial and temporal resolutions in the real atmosphere than models typically resolve, i.e. <1 km. As with all numerical models, the representation of sub-grid scale processes requires parameterization. At typical scales considered, characterization of mixed phase processes within a condensing cloud depends on both cloud microphysics and kinematics of the surrounding atmosphere. Replicating cloud physics at the multi-kilometer scale requires empiricism. The 30+ cloud microphysics parameterization options in the research version of WRF (Skamarock et al., 2008) vary in the number of classes described (cloud ice, cloud liquid, snow, rain, graupel, hail, etc.), and may or may not accurately resolve changes in hydrometeor phase and horizontal spatial location (due to wind) during precipitation. All microphysical schemes predict cloud water and cloud ice based on internal cloud processes that include a variety of empirical formulations or even simple lookup tables. These schemes vary greatly in their accuracy with “mixed phase” schemes generally producing the most accurate simulations of precipitation phase in complex terrain where much of the water is supercooled (Lin, 2007; Reisner et al., 1998; Thompson et al., 2004; Thompson et al., 2008; Morrison et al., 2005; Zängl, 2007; Kaplan et al., 2012). Comprehensive validation of the microphysical schemes over

606 different land surface types (e. g. warm maritime, flat prairie, etc.) with a focus on different
607 snowfall patterns is lacking. In particular, in transition zones between mountains and plains or
608 along coastlines, the complexity of the microphysics becomes even more extreme due the
609 dynamics and interactions of differing air masses with distinct characteristics. The
610 autoconversion and growth processes from cloud water or ice to hydrometeors contain a strong
611 component of empiricism, and in particular, the nucleation media and their chemical
612 composition. Different microphysical parameterizations lead to different spatial distributions of
613 precipitation and produce varying vertical distributions of hydrometeors (Gilmore et al., 2004).
614 Regardless, precipitation rates for each grid cell are averages requiring hydrological modelers to
615 consider the effects of elevation, aspect, etc. in resolving precipitation phase fractions for finer-
616 scale models.
617
618 Numerical models that contain sophisticated cloud microphysics schemes allow assimilation of
619 additional remote sensing data beyond conventional synoptic/large scale observations (balloon
620 data). This is because the coarse spatial and temporal nature of radiosonde data results in the
621 atmosphere being sensed imperfectly/incompletely compared with the scale of motion that
622 weather simulation models can numerically resolve. These observational inadequacies are
623 exacerbated in complex terrain, where precipitation phase fraction can vary on small scales and
624 radar can be blocked by topography and therefore rendered useless in the model initialization.
625 Accurate generation of liquid and frozen precipitation from vapor requires accurate depiction of
626 initial atmospheric moisture conditions (Kalnay and Cai, 2003; Lewis et al., 2006). In
627 acknowledgement of the difficulty and uncertainty of initializing numerical simulation models,
628 atmospheric modelers use the term “bogusing” to describe incorporation of individual
629 observations at a point location into large scale initial conditions in an effort to enhance the
630 accuracy of the simulation (Eddington, 1989). They also employ complex assimilation
631 methodologies to force the early period of the model solutions during the time integration
632 towards fine scale observations (Kalnay and Cai, 2003; Lewis et al., 2006). These asynoptic or
633 fine scale data sources often substantially improve the accuracy of the simulations as time
634 progresses.
635

Hydrologists are increasingly using output from atmospheric models to drive hydrologic models from daily to climatic or multi-decadal timescales (Tung and Haith, 1995; Pachauri, 2002; Wood et al., 2004; Rojas et al., 2011; Yucel et al., 2015). These atmospheric models suffer from the same data paucity and scale issues that likewise challenge the implementation and validation of hydrologic models. Uncertainties in their output, including precipitation volume and phase, begins with the initialization of the atmospheric model from measurements, increases with model choice and microphysics as well as turbulence parameterizations, and is a strong function of the scale of the model. The significance of these uncertainties varies by application, but should be acknowledged. Furthermore, these uncertainties are highly variable in character and magnitude from day to day and location to location. Thus, there has been very little published concerning how well atmospheric models predict precipitation phase. Finally, lack of ground measurements leaves hydrologists with no means to assess and validate atmospheric model predictions.

5. Research Gaps

The incorrect prediction of precipitation phase leads to cascading effects on hydrological simulations (Figure 1). Meeting the challenge of accurately predicting precipitation phase requires the closing of several critical research gaps (Figure 4). Perhaps the most pressing challenge for improving PPM is developing and employing new and improved sources of data. However, new data sources will not yield much benefit without effective incorporation into predictive models (Figure 4). Additionally, both the scientific and management communities lack data products that can be readily understood and broadly used. Addressing these research gaps requires simultaneous engagement both within and between the hydrology and atmospheric observation and modeling communities. Changes to atmospheric temperature and humidity profiles from regional climate change will likely challenge conventional precipitation phase prediction in ways that demand additional observations and improved forecasts.

We also highlight research gaps to improve relatively simple hydrological models without adding unnecessary complexity associated with sophisticated PPM approaches. For example, more efforts to verify the existing PPM in different climatic environments and during specific hydrometeorological events could help determine various temperature thresholds (Table 1) to apply in existing models (section 5.3). In addition, developing gridded precipitation phase

products may eliminate the need to make existing models more complex by applying more complex PPM outside of those models, e.g. similar to precipitation distribution in existing gridded products used by many hydrological models. Ultimately, recognizing the sensitivity of hydrological model outcomes to PPM and identifying what climates and applications require higher phase prediction accuracy are crucial steps to determining the complexity of PPM required for specific applications.

5.1 Conduct focused field campaigns

Intensive field campaigns are extremely effective approaches to address fundamental research gaps focused on the discrimination between rain, snow, and mixed-phase precipitation at the ground by providing opportunities to test novel sensors, collect detailed datasets to develop remote sensing retrieval algorithms and improve PPM estimation methods. The recent Global Precipitation Measurement (GPM) Cold Season Precipitation Experiment (GCPEx) is an example of such a campaign in non-complex terrain where simultaneous observations using arrays of both airborne and ground-based sensors were used to measure and characterize both solid and liquid precipitation (e.g. Skofronick-Jackson et al., 2015). Similar intensive field campaigns are needed in complex terrain that is frequently characterized by highly dynamic and spatially variable hydrometeorological conditions. Such campaigns are expensive to conduct, but can be implemented as part of operational nowcasting to develop rich data resources to advance scientific understanding as was very effectively done during the Vancouver Olympic Games in 2010 (Isaac et al., 2014; Joe et al., 2014). The research community should utilize existing datasets and capitalize on similar opportunities and expand environmental monitoring networks to simultaneously advance both atmospheric and hydrological understanding, especially in complex terrain spanning the rain-snow transition zone.

5.2 Incorporate humidity information

Atmospheric humidity affects the energy budget of falling hydrometeors (Section 4.1), but is rarely considered in precipitation phase prediction. The difficulty in incorporating humidity mainly arises from a lack of observations, both as point measurements and distributed gridded products. For example, while some reanalysis products have humidity information (i.e. National Centers for Environmental Prediction, NCEP reanalysis) they are at spatial scales (i.e. > 1

degree) that are too coarse for resolving precipitation phase in complex topography. Addition of high-quality aspirated humidity sensors at snow monitoring stations, such as the SNOTEL network, would advance our understanding of humidity and its effects on precipitation phase in the mountains. Because dry air masses have regional variations controlled by storm tracks and proximity to water bodies, sensitivity of precipitation phase to humidity variations driven by regional warming remains relatively unexplored.

Although humidity datasets are relatively rare in mountain environments, some gridded data products exist that can be used to investigate the importance of humidity information. Most interpolated gridded data products either do not include any measure of humidity (e.g. Daymet or WorldClim) or use daily temperature measurements to infer humidity conditions (e.g. PRISM). In complex terrain, air temperature can also vary dramatically at relatively small scales from ridgetops to valley bottoms due to cold air drainage (Whiteman et al., 1999) and hence can introduce errors into inferential techniques such as these. Potentially more useful are data assimilation products, such as NLDAS-2, that provide humidity and temperature values at $1/8^{th}$ of a degree scale over the continental U.S. In addition, several data reanalysis products are often available at 1 to 3 year lags from present, including NCEP/NCAR, NARR, and the 20^{th} Century reanalysis. Given the relatively sparse observations of humidity in mountain environments, the accuracy of gridded humidity products is rarely rigorously evaluated (Abatzoglou, 2013). More work is needed to understand the added skill provided by humidity datasets for predicting precipitation phase and its distribution over time and space.

5.2 Incorporate atmospheric information

We echo the call of Feiccabrino et al. (2015) for greater incorporation of atmospheric information into phase prediction and additional verification of the skill in phase prediction provided by atmospheric information.

Several avenues exist to better incorporate atmospheric information into precipitation phase prediction, including direct observations, remote sensing observations, and synthetic products. Radiosonde measurements made daily at many airports and weather forecasting centers have shown some promise for supplying atmospheric profiles of temperature and humidity (Froidurot

et al., 2014). However, these data are only useful to initialize the larger scale structure of temperature and water vapor, and may not capture local-scale variations in complex terrain. It is also their lack of temporal and spatial frequency that prevents their use in accurate precipitation phase prediction, which is inherently a mesoscale problem, i.e., scales of motion <100 km. Atmospheric information on the bright-band height from Doppler radar has been utilized for predicting the altitude of the rain-snow transition (Lundquist et al., 2008; Minder, 2010), but has rarely been incorporated into hydrological modeling applications (Maurer and Mass, 2006; Mizukami et al., 2013). In addition to atmospheric observations, modeling products that assimilate observations or are fully physically-based may provide additional information for precipitation phase prediction. Numerous reanalysis products (described in Section 2.2) provide temperature and humidity at different pressure levels within the atmosphere. To our knowledge, information from reanalysis products has yet to be incorporated into precipitation phase prediction for hydrological applications. Bulk microphysical schemes used by meteorological models (e.g. WRF) provide physically-based estimates of precipitation phase. These schemes capture a wide-variety of processes, including evaporation, sublimation, condensation, and aggradation, and output between two and ten precipitation types. Historically, meteorological models have not been run at spatial scales capable of resolving convective dynamics (e.g. <2 km), which can exacerbate error in precipitation phase prediction in complex terrain with a moist neutral atmosphere. Coarse meteorological models also struggle to produce pockets of frozen precipitation from advection of moisture plumes between mountain ranges and cold air wedged between topographic barriers. However, reduced computational restrictions on running these models at finer spatial scales and over large geographic extents (Rasmussen et al., 2012) are enabling further investigations into precipitation phase change under historical and future climate scenarios. This suggests that finer dynamical downscaling is necessary to resolve precipitation phase which is consistent with similar work attempting to resolve winter precipitation amount in complex terrain (Gutmann et al., 2012). A potentially impactful area of research is to integrate this information into novel approaches to improve precipitation phase prediction skill.

5.3 Disdrometer networks operating at high temporal resolutions

An increase in the types and reliability of disdrometers over the last decade has provided a new suite of tools to more directly measure precipitation phase. Despite this new potential resource

for distinguishing snow and rain, very limited deployments of disdrometers have occurred at the scale necessary to improve hydrologic modeling and rain-snow elevation estimates. The lack of disdrometer deployment likely arises from a number of potential limitations: 1) known issues with accuracy, 2) cost of these systems, and 3) power requirements needed for heating elements. These limitations are clearly a factor in procuring large networks and deploying disdrometers in complex terrain that is remote and frequently difficult to access. However, we advise that disdrometers offer numerous benefits that cannot be substituted with other measurements: 1) they operate at fine temporal scales, 2) they operate in low light conditions that limit other direct observations, and 3) they provide land surface observations rather than precipitation phase in the atmosphere (as compared to more remote methods). Moreover, improvements in disdrometer and power supply technologies that address these limitations would remove restrictions on increased disdrometer deployment.

Transects of disdrometers spanning the rain-snow elevations of key mountain areas could add substantially to both prediction of precipitation phase for modeling purposes, as well as validating typical predictive models. We advocate for transects over key mountain passes where power is generally available and weather forecasts for travel are particularly important. In addition, co-locating disdrometers at long-term research stations where precipitation phase observations could be tied to micro-meteorological and hydrological observations has distinct advantages. These areas often have power supplies and instrumentation expertise to operate and maintain disdrometer networks.

5.4 Compare different indirect phase measurement methods

There is an important need to evaluate the accuracy of different PPM to assess tradeoffs between model complexity and skill (Figure 4). Given the potential for several types of observations to improve precipitation phase prediction (section 5.1-5.3), quantifying the relative skill provided by these different lines of evidence is a critical research gap. Although assessing relative differences between methods is potentially informative, comparison to ground truth measurements is critical for assessing accuracy. Disdrometer measurements and video imaging (Newman et al., 2009) are ideal ground truthing methods that can be employed at fine time steps and under a variety of conditions (section 5.3). Less ideal for accuracy assessment studies are

direct visual observations that are harder to collect at fine time steps and in low light conditions. Similarly, employing coupled observations of precipitation and snow depth has been used to assess accuracy of different precipitation phase prediction methods (Marks et al., 2013; Harder and Pomeroy, 2013), but accuracy assessment of these techniques themselves are lacking under a wide range of contrasting hydrometeorological conditions.

A variety of accuracy assessments are needed that will require co-located distributed measurements. One critical accuracy assessment involves the consistency of different precipitation phase prediction methods under different climate and atmospheric conditions. Assessing the effects of climate and atmospheric conditions requires measurements from a variety of sites covering a range of hydroclimatic conditions and record lengths that span the conceivable range of atmospheric conditions at a given site. Another important evaluation metric is the performance over different time steps. Harder and Pomeroy (2013) showed that hydrometeor and temperature-based prediction methods had errors that substantially decreased across shorter time steps. Identifying the effects of time step length on the accuracy of different prediction methods has been relatively unexplored, but is critical to select the most appropriate method for specific hydrological applications. Finally, the performance metrics used to assess accuracy should be carefully considered. The applications of precipitation phase prediction methods are diverse, necessitating a wide variety of performance metrics, including the probability of snow versus rain (Dai, 2008), the error in annual or total snow/rain accumulation (Rajagopal and Harpold, 2016), performance under extreme conditions of precipitation amount and intensity, determination of the snow-rain elevation (Marks et al., 2013), and uncertainty arising from measurement error and accuracy. Comparison of different metrics across a wide-variety of sites and conditions is lacking but is greatly needed to advance hydrologic science in cold regions.

5.5 Develop spatially resolved products

Many hydrological applications will benefit from gridded data products that are easily integrated into standard hydrological models. Currently, very few options exist for gridded data precipitation phase products. Instead, most hydrological models have some type of submodel or simple scheme that specifies precipitation phase as rain, snow, or mixed-phase precipitation (see

822 Section 4). While testing PPM with ground based observations could lead to improved
823 submodels, we believe development of gridded forcing data may be an easier and more effective
824 solution for many hydrological modeling applications.
825
826 Gridded data products could be derived from a combination of remote sensing and existing
827 synthetic products, but would need to be extensively evaluated. The NASA GPM mission is
828 beginning to produce gridded precipitation phase products at 3-hour and 0.1 degree resolution.
829 However, GPM phase is measured at the top of the atmosphere, typically relies on simple
830 temperature-thresholds, and has yet to be validated with ground based observations. Another
831 existing product is the Snow Data Assimilation System (SNODAS) that estimates liquid and
832 solid precipitation at the 1 km scale. However, the developers of SNODAS caution that it is not
833 suitable for estimating storm totals or regional differences. Furthermore, to our knowledge the
834 precipitation phase product from SNODAS has not been validated with ground observations. We
835 suggest the development of new gridded data products that utilize new PPM (i.e. Harder and
836 Pomeroy, 2013) and new and expanded observational datasets, such as atmospheric information
837 and radar estimates. We advocate for the development of multiple gridded products that can be
838 evaluated with surface observations to compare and contrast their strengths. Accurate gridded
839 phase products rely on the ability to represent the physics of water vapor and energy flows in
840 complex terrain (e.g. Holden et al., 2010) where statistical downscaling methods are typically
841 insufficient (Gutmann et al., 2012). This would also allow for ensembles of phase estimates to be
842 used in hydrological models, similar to what is currently being done with gridded precipitation
843 estimates.
844
845 5.6 Characterization of regional variability and response to climate change
846 The inclusion of new datasets, better validation of PPM, and development of gridded data
847 products will poise the hydrologic community to improve hydrological predictions and better
848 quantify regional sensitivity of phase change to climate changes. Because broad-scale techniques
849 applied to assess changes in precipitation phase and snowfall have relied on temperature, both
850 regionally (Klos et al., 2014; Pierce and Cayan, 2013; Knowles et al., 2006) and globally
851 (Kapnick and Delworth, 2013; O'Gorman, 2014), they have not fully considered the potential
852 non-linearities created by the absence of wet bulb depressions and humidity in assessment of

sensitivity to changes in phase. Consequently, the effects of changes from snow to rain from warming and corresponding changes in humidity will be difficult to predict with current PPM. Recent efforts by Rajagopal and Harpold (2016) have demonstrated that simple temperature thresholds are insufficient to characterize snow-rain transition across the western U.S. (Figure 3), perhaps because of differences in humidity. An increased focus on future humidity trends, patterns, GCM simulation errors (Pierce et al., 2013) and availability of downscaled humidity products at increasingly finer scales (e.g.: Abatzoglou, 2013; Pierce and Cayan, 2016) will enable detailed assessments of the relative role of temperature and humidity in future precipitation phase changes. Recent remote sensing platforms, such as GPM, may offer an additional tool to assess regional variability, however, the current GPM precipitation phase product relies on wet bulb temperatures based on model output and not microwave-based observations (Huffman et al., 2015). In addition to issues with either spatial or temporal resolution or coverage, one of the main challenges in using remotely sensed data for distinguishing between frozen and liquid hydrometeors is the lack of validation. Where products have been validated, the results are usually only relevant for the locale of the study area. Spaceborne radar combined with ground-based radar offers perhaps the most promising solution, but given the non-unique relationship between radar reflectivity and snowfall, further testing is necessary in order to develop reliable algorithms.

Future work is needed to improve projections of changes in snowpack and water availability from regional to global scales. This local to sub-regional characterization is needed for water resource prediction and to better inform decision and policy makers. In particular, the ability to predict the transitional rain-snow elevations and its uncertainty is critical for a variety of end-users, including state and municipal water agencies, flood forecasters, agricultural water boards, transportation agencies, and wildlife, forest, and land managers. Fundamental advancements in characterizing regional variability are possible by addressing the research challenges detailed in sections 5.1-5.5.

6. Conclusions

This review paper is a step towards communicating the potential bottlenecks in hydrological modeling caused by poor representation of precipitation phase (Figure 1). Our goals are to

884 demonstrate that major research gaps in our ability to PPM are contributing to errors and
885 reducing the predictive skill of hydrological models. By highlighting the research gaps that could
886 advance the science of PPM, we provide a roadmap for future advances (Figure 4). While many
887 of the research gaps are recognized by the community and are being pursued, including
888 incorporating atmospheric and humidity information, others remain essentially unexplored (e.g.
889 production of gridded data, widespread ground validation, and remote sensing validation).
890
891 The key points that must be communicated to the hydrologic community and its funding
892 agencies can be distilled into the following two statements: 1) current PPM are too simple to
893 capture important processes and are not well-validated for most locations, 2) the lack of
894 sophisticated PPM increases the uncertainty in estimation of hydrological sensitivity to changes
895 in precipitation phase at local to regional scales. We advocate for better incorporation of new
896 information (5.1-5.2) and improved validation methods (5.3-5.4) to advance our current PPM
897 and observations. These improved PPM and remote-sensing observations will be capable of
898 developing gridded datasets (5.5) and providing new insight that reduce the uncertainty of
899 predicting regional changes from snow to rain (5.6). Improved PPM and existing phase products
900 will also facilitate improvement of simpler hydrological models for which more complex PPM
901 are not justified. A concerted effort by the hydrological and atmospheric science communities to
902 address the PPM challenge will remedy current limitations in hydrological modeling of
903 precipitation phase, advance of understanding of cold regions hydrology, and provide better
904 information to decision makers.
905
906 Acknowledgements
907 This work was conducted as a part of an Innovation Working Group supported by the Idaho,
908 Nevada, and New Mexico EPSCoR Programs and by the National Science Foundation under
909 award numbers IIA-1329469, IIA-1329470 and IIA-1329513. Adrian Harpold was partially
910 supported by USDA NIFA NEV05293. Adrian Harpold and Rina Schumer were supported by
911 the NASA EPSCOR Cooperative Agreement #NNX14AN24A. Timothy Link was partially
912 supported by the Department of the Interior Northwest Climate Science Center (NW CSC)
913 through a Cooperative Agreement #G14AP00153 from the United States Geological Survey
914 (USGS). Seshadri Rajagopal was partially supported by research supported by NSF/USDA grant

915 (#1360506/#1360507) and startup funds provided by Desert Research Institute. The contents of
916 this manuscript are solely the responsibility of the authors and do not necessarily represent the
917 views of the NW CSC or the USGS. This manuscript is submitted for publication with the
918 understanding that the United States Government is authorized to reproduce and distribute
919 reprints for Governmental purposes.

References:

Abatzoglou, J. T.: Development of gridded surface meteorological data for ecological applications and modelling, International Journal of Climatology, 33, 121-131, 10.1002/joc.3413, 2013.

Anderson, E., 2006, Snow Accumulation and Ablation Model – Snow-17, available online at http://www.nws.noaa.gov/oh/hrl/nwsrfs/users_manual/part2/_pdf/22snow17.pdf, accessed August, 2016.

Arkin, P. A., and Ardanuy, P. E.: Estimating climatic-scale precipitation from space: a review, J. Climate, 2, 1229-1238, 1989.

Arnold, J.G., Kiniry, J.R., Srinivasan R., Williams, J.R, Haney, E.B., and Neitsch S.L., 2012, SWAT Input/Output Documentation, Texas Water Resources Institute, TR-439, available online at http://swat.tamu.edu/media/69296/SWAT-IO-Documentation-2012.pdf, accessed August, 2016.

Bales, R. C., Molotch, N. P., Painter, T. H., Dettinger, M. D., Rice, R., and Dozier, J.: Mountain hydrology of the western United States, Water Resources Research, 42, 10.1029/2005wr004387, 2006.

Barnett, T. P., Adam, J. C., and Lettenmaier, D. P.: Potential impacts of a warming climate on water availability in snow-dominated regions, Nature, 438, 303-309, 10.1038/nature04141, 2005.

Battaglia, A., Rustemeier, E., Tokay, A., Blahak, U., and Simmer, C.: PARSIVEL Snow Observations: A Critical Assessment, Journal of Atmospheric and Oceanic Technology, 27, 333-344, 10.1175/2009jtecha1332.1, 2010.

Berghuijs, W. R., Woods, R. A., and Hrachowitz, M.: A precipitation shift from snow towards rain leads to a decrease in streamflow, Nature Climate Change, 4, 583-586, 10.1038/nclimate2246, 2014.

Bernauer, F., Hurkamp, K., Ruhm, W., and Tschiersch, J.: Snow event classification with a 2D video disdrometer - A decision tree approach, Atmospheric Research, 172, 186-195, 2016.

947 Bergström, S. 1995. The HBV model. In: Singh, V.P. (Ed.) Computer Models of Watershed
948 Hydrology. Water Resources Publications, Highlands Ranch, CO., pp. 443-476.

949 Berris, S. N., and Harr, R. D.: Comparative snow accumulation and melt during rainfall in
950 forested and clear-cut plots in the Western Cascades of Oregon, Water Resources Research,
951 23, 135-142, 10.1029/WR023i001p00135, 1987.

952 Bicknell, B.R., Imhoff, J.C., Kittle, J.L., Jr., Donigian, A.S., Jr., and Johanson, R.C.,
953 Hydrological Simulation Program--Fortran, User's manual for version 11: U.S.
954 Environmental Protection Agency, National Exposure Research Laboratory, Athens, Ga.,
955 EPA/600/R-97/080, 755 p., 1997.

956 Boe, E. T.: Assessing Local Snow Variability Using a Network of Ultrasonic Snow Depth
957 Sensors, Master of Science in Hydrologic Sciences, Geosciences, Boise State, 2013.

958 Boodoo, S., Hudak, D., Donaldson, N., and Leduc, M.: Application of Dual-Polarization Radar
959 Melting-Layer Detection Algorithm, Journal of Applied Meteorology and Climatology, 49,
960 1779-1793, 10.1175/2010jamc2421.1, 2010.

961 Borrmann, S., and Jaenicke, R.: Application of microholography for ground-based in-situ
962 measurements in stratus cloud layers - a case study, Journal of Atmospheric and Oceanic
963 Technology, 10, 277-293, 10.1175/1520-0426(1993)010<0277:aomfgb>2.0.co;2, 1993.

964 Braun, L. N.: Simulation of snowmelt-runoff in lowland and lower alpine regions of Switzerland,
965 Diss. Naturwiss. ETH Zürich, Nr. 7684, 0000. Ref.: Ohmura, A.; Korref.: Vischer, D.;
966 Korref.: Lang, H., 1984.

967 Cao, Q., Hong, Y., Chen, S., Gourley, J. J., Zhang, J., and Kirstetter, P. E.: Snowfall
968 Detectability of NASA's CloudSat: The First Cross-Investigation of Its 2C-Snow-Profile
969 Product and National Multi-Sensor Mosaic QPE (NMQ) Snowfall Data, Progress in
970 Electromagnetics Research-Pier, 148, 55-61, 10.2528/pier14030405, 2014.

971 Cayan, D. R., Kammerdiener, S. A., Dettinger, M. D., Caprio, J. M., and Peterson, D. H.:
972 Changes in the onset of spring in the western United States, Bulletin of the American
973 Meteorological Society, 82, 399-415, 10.1175/1520-0477(2001)082<0399:citoos>2.3.co;2,
974 2001.

975 Chandrasekar, V., Keranen, R., Lim, S., and Moisseev, D.: Recent advances in classification of
976 observations from dual polarization weather radars, Atmospheric Research, 119, 97-111,
977 10.1016/j.atmosres.2011.08.014, 2013.

978 Chen, S., Gourley, J. J., Hong, Y., Cao, Q., Carr, N., Kirstetter, P.-E., Zhang, J., and Flamig, Z.:
979 Using citizen science reports to evaluate estimates of surface precipitation type, Bulletin of
980 the American Meteorological Society, 10.1175/BAMS-D-13-00247.1, 2015.

981 Dai, A.: Temperature and pressure dependence of the rain-snow phase transition over land and
982 ocean, Geophysical Research Letters, 35, 10.1029/2008gl033295, 2008.

983 Ding, B., Yang, K., Qin, J., Wang, L., Chen, Y., and He, X.: The dependence of precipitation
984 types on surface elevation and meteorological conditions and its parameterization, Journal
985 of Hydrology, 513, 154-163, 10.1016/j.jhydrol.2014.03.038, 2014.

986 Eddington, L. W.: Satellite-Derived Moisture-Bogusing Profiles for the North Atlantic Ocean,
987 DTIC Document, 1989.

988 Elmore, K. L.: The NSSL Hydrometeor Classification Algorithm in Winter Surface
989 Precipitation: Evaluation and Future Development, Weather and Forecasting, 26, 756-765,
990 10.1175/waf-d-10-05011.1, 2011.

991 Fang, X., Pomeroy, J. W., Ellis, C. R., MacDonald, M. K., DeBeer, C. M., and Brown, T.: Multi-
992 variable evaluation of hydrological model predictions for a headwater basin in the Canadian
993 Rocky Mountains, Hydrol. Earth Syst. Sci., 17, 1635-1659, 10.5194/hess-17-1635-2013,
994 2013.

995 Fatichi, S., Vivoni, E. R., Ogden, F. L., Ivanov, V. Y., Mirus, B., Gochis, D., Downer, C. W.,
996 Camporese, M., Davison, J. H., Ebel, B., Jones, N., Kim, J., Mascaro, G., Niswonger, R.,
997 Restrepo, P., Rigon, R., Shen, C., Sulis, M., and Tarboton, D.: An overview of current
998 applications, challenges, and future trends in distributed process-based models in hydrology,
999 Journal of Hydrology, 537, 45-60, 2016.

1000 Feiccabrino, J., Lundberg, A., and Gustafsson, D.: Improving surface-based precipitation phase
1001 determination through air mass boundary identification, Hydrology Research, 43, 179-191,
1002 10.2166/nh.2012.060, 2013.

1003 Feiccabrino, J., Gustafsson, D., and Lundberg, A.: Surface-based precipitation phase
1004 determination methods in hydrological models, Hydrology Research, 44, 44-57, 2015.

1005 Floyd, W., and Weiler, M.: Measuring snow accumulation and ablation dynamics during rain-on-
1006 snow events: innovative measurement techniques, Hydrological Processes, 22, 4805-4812,
1007 10.1002/hyp.7142, 2008.

1008 Fritze, H., Stewart, I. T., and Pebesma, E.: Shifts in Western North American Snowmelt Runoff
1009 Regimes for the Recent Warm Decades, Journal of Hydrometeorology, 12, 989-1006,
1010 10.1175/2011jhm1360.1, 2011.

1011 Froidurot, S., Zin, I., Hingray, B., and Gautheron, A.: Sensitivity of Precipitation Phase over the
1012 Swiss Alps to Different Meteorological Variables, Journal of Hydrometeorology, 15, 685-
1013 696, 10.1175/jhm-d-13-073.1, 2014.

1014 Garvelmann, J., Pohl, S., and Weiler, M.: From observation to the quantification of snow
1015 processes with a time-lapse camera network, Hydrology and Earth System Sciences, 17,
1016 1415-1429, 10.5194/hess-17-1415-2013, 2013.

1017 Giangrande, S. E., Krause, J. M., and Ryzhkov, A. V.: Automatic designation of the melting
1018 layer with a polarimetric prototype of the WSR-88D radar, Journal of Applied Meteorology
1019 and Climatology, 47, 1354-1364, 10.1175/2007jamc1634.1, 2008.

1020 Gilmore, M. S., Straka, J. M., and Rasmussen, E. N.: Precipitation Uncertainty Due to Variations
1021 in Precipitation Particle Parameters within a Simple Microphysics Scheme, Monthly
1022 Weather Review, 132, 2610-2627, 10.1175/MWR2810.1, 2004.

1023 Godsey, S. E., Kirchner, J. W., and Tague, C. L.: Effects of changes in winter snowpacks on
1024 summer low flows: case studies in the Sierra Nevada, California, USA, Hydrological
1025 Processes, 28, 5048-5064, 10.1002/hyp.9943, 2014.

1026 Grazioli, J., Tuia, D., and Berne, A.: Hydrometeor classification from polarimetric radar
1027 measurements: a clustering approach, Atmospheric Measurement Techniques, 8, 149-170,
1028 10.5194/amt-8-149-2015, 2015.

1029 Gusev, E.M. and Nasonova, O.N., Parameterization of Heat and Water Exchange on Land
1030 Surface for Coupling Hydrologic and Climate Models, Water Resources., 25(4): 421–431,
1031 1998.

1032 Gutmann, E.D., Rasmussen, R.M., Liu, C., Ikeda, K., Gochis, D., Clark, P.P., Dudhia, J., and
1033 Gregory, T.: A comparison of statistical and dynamical downscaling of winter precipitation
1034 over complex terrain, *Journal of Climate,* 25(1): 262-281, 2012.

1035 Harder, P., and Pomeroy, J.: Estimating precipitation phase using a psychrometric energy
1036 balance method, Hydrological Processes, 27, 1901-1914, 10.1002/hyp.9799, 2013.

1037 Harder, P., and Pomeroy, J. W.: Hydrological model uncertainty due to precipitation-phase
1038 partitioning methods, Hydrological Processes, 28, 4311-4327, 2014.

1039 Hauser, D., Amayenc, P., and Nutten, B.: A new optical instrument for simultaneous
1040 measurement of raindrop diameter and fall speed distributions, Atmos. Oceanic Technol., 1,
1041 256-259, 1984.

1042 HEC-1, 1998, Flood Hydrograph Package, User's Manual, CPD-1A, Version 4.1, available
1043 online at, http://www.hec.usace.army.mil/publications/ComputerProgramDocumentation/HEC-
1044 1_UsersManual_(CPD-1a).pdf, accessed August, 2016.

1045 Hedrick, A. R., and Marshall, H.-P.: Automated Snow Depth Measurements in Avalanche
1046 Terrain Using Time-Lapse Photography, 2014 International Snow Science Workshop, 2014,

1047 Holden, Z. A., Abatzoglou, J. T., Luce, C. H., & Baggett, L. S. Empirical downscaling of daily
1048 minimum air temperature at very fine resolutions in complex terrain. *Agricultural and*
1049 *Forest Meteorology*, *151*, 1066-1073. doi:10.1016/j.agrformet.2011.03.011, 2011.

1050 Hou, A. Y., Kakar, R. K., Neeck, S., Azarbarzin, A. A., Kummerow, C. D., Kojima, M., Oki, R.,
1051 Nakamura, K., and Iguchi, T.: The global precipitation measurement mission, Bulletin of the
1052 American Meteorological Society, 95, 701-722, 2014.

1053 Isaac, G. A., Joe, P. I., Mailhot, J., Bailey, M., Bélair, S., Boudala, F. S., . . . Wilson, L. J.
1054 Science of nowcasting Olympic weather for Vancouver 2010 (SNOW-V10): A World
1055 Weather Research Programme project. Pure and Applied Geophysics, 171(1-2), 1-24.
1056 doi:10.1007/s00024-012-0579-0, 2014.

1057 Jepsen, S. M., Harmon, T. C., Meadows, M. W., and Hunsaker, C. T.: Hydrogeologic influence
1058 on changes in snowmelt runoff with climate warming: Numerical experiments on a mid-
1059 elevation catchment in the Sierra Nevada, USA, Journal of Hydrology, 533, 332-342,
1060 10.1016/j.jhydrol.2015.12.010, 2016.

1061 Joe, P., Scott, B., Doyle, C., Isaac, G., Gultepe, I., Forsyth, D., . . . Boudala, F. The monitoring
1062 network of the Vancouver 2010 Olympics. Pure and Applied Geophysics, 171(1-2), 25-58,
1063 doi:10.1007/s00024-012-0588-z, 2014.

1064 Joss, J., and Waldvogel, A.: Ein Spektograph fuer Niederschlagstropfen mit automatischer
1065 Auswertung, Pure Appl. Geophys, 68, 240--246, 1967.

1066 Kalnay, E., and Cai, M.: Impact of urbanization and land-use change on climate, Nature, 423,
1067 528-531, 10.1038/nature01675, 2003.

1068 Kaplan, M. L., Vellore, R. K., Marzette, P. J., and Lewis, J. M.: The role of windward-side
1069 diabatic heating in Sierra Nevada spillover precipitation, Journal of Hydrometeorology, 13,
1070 1172-1194, 2012.

1071 Kapnick, S. B. and Delworth, T. L.: Controls of global snow under a changed climate, Journal of
1072 Climate, 26, 5537-5562, 2013.

1073 Kidd, C.: On rainfall retrieval using polarization-corrected temperatures, International Journal of
1074 Remote Sensing, 19, 981-996, 10.1080/014311698215829, 1998.

1075 Kidd, C., and Huffman, G.: Global precipitation measurement, Meteorological Applications, 18,
1076 334-353, 10.1002/met.284, 2011.

1077 Kienzle, S. W.: A new temperature based method to separate rain and snow, Hydrological
1078 Processes, 22, 5067-5085, 10.1002/hyp.7131, 2008.

1079 Kim, M. J., Weinman, J. A., Olson, W. S., Chang, D. E., Skofronick-Jackson, G., and Wang, J.
1080 R.: A physical model to estimate snowfall over land using AMSU-B observations, Journal
1081 of Geophysical Research-Atmospheres, 113, 16, 10.1029/2007jd008589, 2008.

1082 Kirchner, J. W.: Getting the right answers for the right reasons: Linking measurements, analyses,
1083 and models to advance the science of hydrology, Water Resources Research, 42,
1084 10.1029/2005wr004362, 2006.

1085 Kite, G. 1995. The HBV model. In: Singh, V.P. (Ed.) Computer Models of Watershed
1086 Hydrology. Water Resources Publications, Highlands Ranch, CO., pp. 443-476.

1087 Klos, P. Z., Link, T. E., and Abatzoglou, J. T.: Extent of the rain-snow transition zone in the
1088 western US under historic and projected climate, Geophysical Research Letters, 41, 4560-
1089 4568, 10.1002/2014gl060500, 2014.

1090 Knollenberg, R. G.: Some results of measurements of latent heat released from seeded stratus,
1091 Bulletin of the American Meteorological Society, 51, 580-&, 1970.

1092 Knowles, N., Dettinger, M. D., and Cayan, D. R.: Trends in snowfall versus rainfall in the
1093 Western United States, Journal of Climate, 19, 4545-4559, 2006.

1094 Kongoli, C., Pellegrino, P., Ferraro, R. R., Grody, N. C., and Meng, H.: A new snowfall
1095 detection algorithm over land using measurements from the Advanced Microwave Sounding
1096 Unit (AMSU), Geophysical Research Letters, 30, 10.1029/2003gl017177, 2003.

1097 Kongoli, C., Meng, H., Dong, J., and Ferraro, R.: A snowfall detection algorithm over land
1098 utilizing high-frequency passive microwave measurements-Application to ATMS, Journal
1099 of Geophysical Research-Atmospheres, 120, 1918-1932, 10.1002/2014jd022427, 2015.

1100 Kruger, A., and Krajewski, W. F.: Two-dimensional video disdrometer: A description, Journal of
1101 Atmospheric and Oceanic Technology, 19, 602-617, 10.1175/1520-
1102 0426(2002)019<0602:tdvdad>2.0.co;2, 2002.

1103 Kulie, M. S., Milani, L., Wood, N. B., Tushaus, S. A., Bennartz, R., and L'Ecuyer, T. S.: A
1104 Shallow Cumuliform Snowfall Census Using Spaceborne Radar, Journal of
1105 Hydrometeorology, 17, 1261-1279, 10.1175/jhm-d-15-0123.1, 2016.

1106 L'hôte, Y., Chevallier, P., Coudrain, A., Lejeune, Y., and Etchevers, P.: Relationship between
1107 precipitation phase and air temperature: comparison between the Bolivian Andes and the
1108 Swiss Alps/Relation entre phase de précipitation et température de l'air: comparaison entre
1109 les Andes Boliviennes et les Alpes Suisses, Hydrological sciences journal, 50, 2005.

1110 Leavesley, G. H., Restrepo, P. J., Markstrom, S. L., Dixon, M., and Stannard, L. G.: The
1111 Modular Modeling System (MMS): User's Manual, U.S. Geological Survey, Denver,
1112 COOpen File Report 96-151, 1996.

1113 Lempio, G. E., Bumke, K., and Macke, A.: Measurement of solid precipitation with an optical
1114 disdrometer, Advances in Geosciences, 10, 91-97, 2007.

1115 Lewis, J., Lakshmivarahan, S., and Dhall, S.: Dynamic Data Assimilation: A Least Squares
1116 Approach, Cambridge Univ. Press, 745 pp., 2006.

1117 Lin, Y.-L.: Mesoscale Dynamics, Cambridge University Press, 630 pp., 2007.

1118 Liu, G.: Deriving snow cloud characteristics from CloudSat observations, Journal of Geophysical
1119 Research-Atmospheres, 113, 10.1029/2007jd009766, 2008.

1120 Loffler-Mang, M., Kunz, M., and Schmid, W.: On the performance of a low-cost K-band
1121 Doppler radar for quantitative rain measurements, Journal of Atmospheric and Oceanic
1122 Technology, 16, 379-387, 10.1175/1520-0426(1999)016<0379:otpoal>2.0.co;2, 1999.

1123 Luce, C. H., and Holden, Z. A.: Declining annual streamflow distributions in the Pacific
1124 Northwest United States, 1948-2006, Geophysical Research Letters, 36,
1125 10.1029/2009gl039407, 2009.

1126 Lundquist, J. D., Neiman, P. J., Martner, B., White, A. B., Gottas, D. J., and Ralph, F. M.: Rain
1127 versus snow in the Sierra Nevada, California: Comparing Doppler profiling radar and
1128 surface observations of melting level, Journal of Hydrometeorology, 9, 194-211,
1129 10.1175/2007jhm853.1, 2008.

1130 Lynch-Stieglitz, M.: The development and validation of a simple snow model for the GISS
1131 GCM, Journal of Climate, 7, 1842-1855, 1994.

1132 Marks, D., Link, T., Winstral, A., and Garen, D.: Simulating snowmelt processes during rain-on-
1133 snow over a semi-arid mountain basin, Annals of Glaciology, 32, 195-202, 2001.

1134 Marks, D., Winstral, A., Reba, M., Pomeroy, J., and Kumar, M.: An evaluation of methods for
1135 determining during-storm precipitation phase and the rain/snow transition elevation at the
1136 surface in a mountain basin, Advances in Water Resources, 55, 98-110,
1137 http://dx.doi.org/10.1016/j.advwatres.2012.11.012, 2013.

1138 Martinec, J., and Rango, A.: Parameter values for snowmelt runoff modelling, Journal of
1139 Hydrology, 84, 197-219, http://dx.doi.org/10.1016/0022-1694(86)90123-X, 1986.

1140 Martinec J., Rango A., Roberts R., 2008, Snowmelt Runoff Model, User's Manual, available
1141 online at http://aces.nmsu.edu/pubs/research/weather_climate/SRMSpecRep100.pdf, accessed
1142 August, 2016.

1143 Matrosov, S. Y., Shupe, M. D., and Djalalova, I. V.: Snowfall retrievals using millimeter-
1144 wavelength cloud radars, Journal of Applied Meteorology and Climatology, 47, 769-777,
1145 10.1175/2007jamc1768.1, 2008.

1146 Maurer, E. P., and Mass, C.: Using radar data to partition precipitation into rain and snow in a
1147 hydrologic model, Journal of Hydrologic Engineering, 11, 214-221, 10.1061/(asce)1084-
1148 0699(2006)11:3(214), 2006.

1149 McCabe, G. J., and Wolock, D. M.:General-circulation-model simulations of future snowpack in
1150 the western United States1. JAWRA Journal of the American Water Resources Association,
1151 35(6), 1473-1484, 1999a.

1152 McCabe, G.J. and Wolock, D.M.: Recent Declines in Western U.S. Snowpack in the Context of
1153 Twentieth-Century Climate Variability, Earth Interactions, 13, 1-15, DOI:
1154 10.1175/2009EI283.1, 1999b.

1155 McCabe, G. J., Clark, M. P., and Hay, L. E.: Rain-on-snow events in the western United States,
1156 Bulletin of the American Meteorological Society, 88, 319-+, 10.1175/bams-88-3-319, 2007.

1157 McCabe, G. J., and Wolock, D. M.: Long-term variability in Northern Hemisphere snow cover
1158 and associations with warmer winters, Climatic Change, 99, 141-153, 2010.

1159 MIKE-SHE User Manual, available online at
1160 ftp://ftp.cgs.si/Uporabniki/UrosZ/mike/Manuals/MIKE_SHE/MIKE_SHE.htm, accessed August,
1161 2016.

1162 Milly, P. C. D., Betancourt, J., Falkenmark, M., Hirsch, R. M., Kundzewicz, Z. W., Lettenmaier,
1163 D. P., and Stouffer, R. J.: Climate change - Stationarity is dead: Whither water
1164 management?, Science, 319, 573-574, 10.1126/science.1151915, 2008.

1165 Minder, J. R.: The Sensitivity of Mountain Snowpack Accumulation to Climate Warming,
1166 Journal of Climate, 23, 2634-2650, 10.1175/2009jcli3263.1, 2010.

1167 Minder, J. R., and Kingsmill, D. E.: Mesoscale Variations of the Atmospheric Snow Line over
1168 the Northern Sierra Nevada: Multiyear Statistics, Case Study, and Mechanisms, Journal of
1169 the Atmospheric Sciences, 70, 916-938, 10.1175/jas-d-12-0194.1, 2013.

1170 Mitchell K., Ek, M., Wong, V., Lohmann, D., Koren, V., Schaake, J., Duan, Q., Gayno, G.,
1171 Moore, B., Grunmann, P., Tarpley, D., Ramsay, B., Chen, F., Kim, J., Pan, H.L., Lin, Y.,
1172 Marshall, C., Mahrt, L., Meyers, T., and Ruscher, P.: 2005, Noah Land-Surface Model,
1173 User's Guide, version 2.7.1, available at
1174 ftp://ftp.emc.ncep.noaa.gov/mmb/gcp/ldas/noahlsm/ver_2.7.1, accessed August, 2016.

1175 Mizukami, N., Koren, V., Smith, M., Kingsmill, D., Zhang, Z. Y., Cosgrove, B., and Cui, Z. T.:
1176 The Impact of Precipitation Type Discrimination on Hydrologic Simulation: Rain-Snow
1177 Partitioning Derived from HMT-West Radar-Detected Brightband Height versus Surface
1178 Temperature Data, Journal of Hydrometeorology, 14, 1139-1158, 10.1175/jhm-d-12-035.1,
1179 2013.

1180 Morrison, H., Curry, J., and Khvorostyanov, V.: A new double-moment microphysics
1181 parameterization for application in cloud and climate models. Part I: Description, Journal of
1182 the Atmospheric Sciences, 62, 1665-1677, 2005.

1183 Motoyama, H.: Simulation of seasonal snowcover based on air temperature and precipitation,
1184 Journal of Applied Meteorology, 29, 1104-1110, 1990.

1185 Newman, A. J., Kucera, P. A., & Bliven, L. F.. Presenting the snowflake video imager (SVI).
1186 Journal of Atmospheric and Oceanic Technology, 26(2), 167-179, 2009.
1187 doi:10.1175/2008jtecha1148.1

1188 NOAA, 2016. NEXRAD Data Archive, Inventory and Access, available online at
1189 https://www.ncdc.noaa.gov/nexradinv/ accessed 11/10/2016

1190 Noh, Y. J., Liu, G. S., Jones, A. S., and Haar, T. H. V.: Toward snowfall retrieval over land by
1191 combining satellite and in situ measurements, Journal of Geophysical Research-
1192 Atmospheres, 114, 10.1029/2009jd012307, 2009.

1193 O'Gorman, P.A.: Contrasting responses of mean and extreme snowfall to climate change,
1194 Nature, 512, 416-418, 2014.

1195 Olsen, A.: Snow or rain?—A matter of wet-bulb temperature, thesis, Uppsala Univ., Uppsala,
1196 Sweden.(Available at http://www. geo. uu. se/luva/exarb/2003/Arvid_Olsen. pdf), 2003.

Olson, W. S., Kummerow, C. D., Heymsfield, G. M., and Giglio, L.: A method for combined passive-active microwave retrievals of cloud and precipitation profiles, Journal of Applied Meteorology, 35, 1763-1789, 10.1175/1520-0450(1996)035<1763:amfcpm>2.0.co;2, 1996.

Pachauri, R. K.: Intergovernmental panel on climate change (IPCC): Keynote address, Environmental Science and Pollution Research, 9, 436-438, 2002.

Pagano, T. C., Wood, A. W., Ramos, M. H., Cloke, H. L., Pappenberger, F., Clark, M. P., Cranston, M., Kavetski, D., Mathevet, T., Sorooshian, S., and Verkade, J. S.: Challenges of Operational River Forecasting, Journal of Hydrometeorology, 15, 1692-1707, 10.1175/jhm-d-13-0188.1, 2014.

Parajka, J., Haas, P., Kirnbauer, R., Jansa, J., and Bloeschl, G.: Potential of time-lapse photography of snow for hydrological purposes at the small catchment scale, Hydrological Processes, 26, 3327-3337, 10.1002/hyp.8389, 2012.

Park, H., Ryzhkov, A. V., Zrnic, D. S., and Kim, K.-E.: The Hydrometeor Classification Algorithm for the Polarimetric WSR-88D: Description and Application to an MCS, Weather and Forecasting, 24, 730-748, 10.1175/2008waf2222205.1, 2009.

Pierce, D. W. and Cayan, D. R.: The uneven response of different snow measures to human-induced climate warming. Journal of Climate, 26, 4148-4167, 2013.

Pierce, D. W., Westerling, A. L., & Oyler, J.. Future humidity trends over the western united states in the CMIP5 global climate models and variable infiltration capacity hydrological modeling system. Hydrology and Earth System Sciences, 17(5), 1833-1850, 2013.

Pierce, D. W. and Cayan, D. R. Downscaling humidity with localized constructed analogs (LOCA) over the conterminous united states. Climate Dynamics, 47, 411-431, 2016.

Pipes, A., and Quick, M. C.: UBC watershed model users guide, Department of Civil Engineering, University of British Columbia, 1977.

Rajagopal, S., and Harpold, A.: Testing and Improving Temperature Thresholds for Snow and Rain Prediction in the Western United States, Journal of American Water Resources Association, 2016.

1224 Rasmussen, R., Baker, B., Kochendorfer, J., Meyers, T., Landolt, S., Fischer, A. P., Black, J.,
1225 Thériault, J. M., Kucera, P., Gochis, D., Smith, C., Nitu, R., Hall, M., Ikeda, K., and
1226 Gutmann, E.: How Well Are We Measuring Snow: The NOAA/FAA/NCAR Winter
1227 Precipitation Test Bed, Bulletin of the American Meteorological Society, 93, 811-829,
1228 10.1175/BAMS-D-11-00052.1, 2012.

1229 Reisner, J., Rasmussen, R. M., and Bruintjes, R.: Explicit forecasting of supercooled liquid water
1230 in winter storms using the MM5 mesoscale model, Quarterly Journal of the Royal
1231 Meteorological Society, 124, 1071-1107, 1998.

1232 Rojas, R., Feyen, L., Dosio, A., and Bavera, D.: Improving pan-European hydrological
1233 simulation of extreme eventsthrough statistical bias correction of RCM-driven
1234 climatesimulations, Hydrology and Earth System Sciences, 15, 2599, 2011.

1235 Safeeq, M., Mauger, G. S., Grant, G. E., Arismendi, I., Hamlet, A. F., and Lee, S. Y.: Comparing
1236 Large-Scale Hydrological Model Predictions with Observed Streamflow in the Pacific
1237 Northwest: Effects of Climate and Groundwater, Journal of Hydrometeorology, 15, 2501-
1238 2521, 10.1175/jhm-d-13-0198.1, 2014.

1239 Sevruk, B.: Assessment of snowfall proportion in monthly precipitation in Switzerland, Zbornik
1240 meteoroloskih i Hidroloskih Radovav Beograd, 10, 315-318, 1984.

1241 Shamir, E., and Georgakakos, K. P.: Distributed snow accumulation and ablation modeling in the
1242 American River basin, Advances in Water Resources, 29, 558-570,
1243 10.1016/j.advwatres.2005.06.010, 2006.

1244 Skamarock, W. C., Klemp, J. B., Dudhia, J., Gill, D. O., Barker, D. M., Duda, M. G., Huang, X.-
1245 Y., Wang, W., and Powers, J. G.: A description of the advanced research WRF version
1246 3NCAR Tech. Note NCAR/TN-475+STR, 113, 2008.

1247 Skofronick-Jackson, G., Hudak, D., Petersen, W., Nesbitt, S. W., Chandrasekar, V., Durden, S.,
1248 Gleicher, K. J., Huang, G.-J., Joe, P., Kollias, P., Reed, K. A., Schwaller, M. R., Stewart, R.,
1249 Tanelli, S., Tokay, A., Wang, J. R., and Wolde, M.: Global Precipitation Measurement Cold
1250 Season Precipitation Experiment (GCPEX): For Measurement's Sake, Let It Snow, Bulletin
1251 of the American Meteorological Society, 96, 1719-1741, doi:10.1175/BAMS-D-13-00262.1,
1252 2015.

SNTHERM Online Documentation, available at http://www.geo.utexas.edu/climate/Research/SNOWMIP/SUPERSNOW2/rjordan.html, accessed August, 2016.

Stewart, R. E.: Precipitation Types in the Transition Region of Winter Storms, Bulletin of the American Meteorological Society, 73, 287-296, 10.1175/1520-0477(1992)073<0287:PTITTR>2.0.CO;2, 1992.

Stewart, R. E., Theriault, J. M., and Henson, W.: On the Characteristics of and Processes Producing Winter Precipitation Types near 0 degrees C, Bulletin of the American Meteorological Society, 96, 623-639, 10.1175/bams-d-14-00032.1, 2015.

Tague, C.L, and Band, L.E.: RHESSys: Regional Hydro-Ecologic Simulation System—An Object Oriented Approach to Spatially Distributed Modeling of Carbon, Water, and Nutrient Cycling, Earth Interactions, 8, 19, 1-42, 2004.

Tarboton, D.G., and Luce, C.H., 1996, Utah Energy Balance Snow Accumulation and Melt Model (UEB), available online at http://www.fs.fed.us/rm/boise/publications/watershed/rmrs_1996_tarbotond001.pdf, accessed August, 2016.

Tarboton, D., Jackson, T., Liu, J., Neale, C., Cooley, K., and McDonnell, J.: A Grid Based Distributed Hydrologic Model: Testing Against Data from Reynolds Creek Experimental Watershed, Preprints AMS Conf. on Hydrol, 79-84, 1995.

Theriault, J. M., and Stewart, R. E.: On the effects of vertical air velocity on winter precipitation types, Natural Hazards and Earth System Sciences, 7, 231-242, 2007.

Theriault, J. M., and Stewart, R. E.: A Parameterization of the Microphysical Processes Forming Many Types of Winter Precipitation, Journal of the Atmospheric Sciences, 67, 1492-1508, 10.1175/2009jas3224.1, 2010.

Theriault, J. M., Stewart, R. E., and Henson, W.: On the Dependence of Winter Precipitation Types on Temperature, Precipitation Rate, and Associated Features, Journal of Applied Meteorology and Climatology, 49, 1429-1442, 10.1175/2010jamc2321.1, 2010.

1280 Theriault, J. M., Stewart, R. E., and Henson, W.: Impacts of terminal velocity on the trajectory of
1281 winter precipitation types, Atmospheric Research, 116, 116-129,
1282 10.1016/j.atmosres.2012.03.008, 2012.

1283 Thompson, E. J., Rutledge, S. A., Dolan, B., Chandrasekar, V., and Cheong, B. L.: A Dual-
1284 Polarization Radar Hydrometeor Classification Algorithm for Winter Precipitation, Journal
1285 of Atmospheric and Oceanic Technology, 31, 1457-1481, 10.1175/jtech-d-13-00119.1,
1286 2014.

1287 Thompson, G., Rasmussen, R. M., and Manning, K.: Explicit forecasts of winter precipitation
1288 using an improved bulk microphysics scheme. Part I: Description and sensitivity analysis,
1289 Monthly Weather Review, 132, 519-542, 2004.

1290 Thompson, G., Field, P. R., Rasmussen, R. M., and Hall, W. D.: Explicit forecasts of winter
1291 precipitation using an improved bulk microphysics scheme. Part II: Implementation of a
1292 new snow parameterization, Monthly Weather Review, 136, 5095-5115, 2008.

1293 Todini, E.: The ARNO Rainfall-runoff model, Journal of Hydrology, 175, 339-382, 1996.

1294 Tung, C.-P., and Haith, D. A.: Global-warming effects on New York streamflows, Journal of
1295 Water Resources Planning and Management, 121, 216-225, 1995.

1296 U.S. Army Corps of Engineers: Summary Report of the Snow Investigation Hydrological
1297 Practices, 3rd Edition, Chapter 2, 54-56, North Pacific Division, Portland, Oregon, 1956.

1298 Verseghy, D., 2009, CLASS-The Canadian Land Surface Scheme, Version 3.4, Technical
1299 Documentation, Version 1.1, Environment Canada, available online at
1300 http://www.usask.ca/ip3/download/CLASS_v3_4_Documentation_v1_1.pdf, accessed
1301 August, 2016.

1302 VIC Documentation, available online at https://vic.readthedocs.io/en/develop/, accessed August,
1303 2016.

1304 Wang, R., Kumar, M., and Marks, D. Anomalous trend in soil evaporation in a semi-arid, snow-
1305 dominated watershed. Advances in Water Resources, 57, 32-40, 2013.

1306 Wang, R., Kumar, M., and Link, T. E.: Potential trends in snowmelt generated peak streamflows
1307 in a warming climate, Geophys. Res. Lett. 43, 10.1002/ 2016GL068935, 2016.

Wen, L., Nagabhatla, N., Lu, S., and Wang, S.-Y.: Impact of rain snow threshold temperature on snow depth simulation in land surface and regional atmospheric models, Advances in Atmospheric Sciences, 30, 1449-1460, 10.1007/s00376-012-2192-7, 2013.

White, A. B., Gottas, D. J., Strem, E. T., Ralph, F. M., and Neiman, P. J.: An automated brightband height detection algorithm for use with Doppler radar spectral moments, Journal of Atmospheric and Oceanic Technology, 19, 687-697, 10.1175/1520-0426(2002)019<0687:aabhda>2.0.co;2, 2002.

White, A. B., Gottas, D. J., Henkel, A. F., Neiman, P. J., Ralph, F. M., and Gutman, S. I.: Developing a Performance Measure for Snow-Level Forecasts, Journal of Hydrometeorology, 11, 739-753, 10.1175/2009jhm1181.1, 2010.

Whiteman, C. D., Bian, X., & Zhong, S.. Wintertime evolution of the temperature inversion in the colorado plateau basin. *Journal of Applied Meteorology*, *38*(8), 1103-1117, 1999.

Wigmosta, M.S., Vail, L.W., and Lettenmaier, D.P.: A distributed hydrology-vegetation model for complex terrain, Water Resources Research, 30(6), 1665-1679, 1994.

Wilheit, T. T., Chang, A. T. C., King, J. L., Rodgers, E. B., Nieman, R. A., Krupp, B. M., Milman, A. S., Stratigos, J. S., and Siddalingaiah, H.: Microwave radiometric observation nea 19.35, 92 and 183 GHz of precipitation in tropical storm Cora, Journal of Applied Meteorology, 21, 1137-1145, 10.1175/1520-0450(1982)021<1137:mronag>2.0.co;2, 1982.

Wood, A. W., Leung, L. R., Sridhar, V., and Lettenmaier, D.: Hydrologic implications of dynamical and statistical approaches to downscaling climate model outputs, Climatic change, 62, 189-216, 2004.

Wood, N., L'Ecuyer, T. S., Vane, D., Stephens, G., and Partain, P.: Level 2C snow profile process description and interface control document, 2013.

Yamazaki, T.: A One-dimensional Land Surface Model Adaptable to Intensely Cold Regions and its Applications in Eastern Siberia, 79, 1107-1118, 2001.

Yang Z.L., Dickinson, R.E., Robock, A. and Vinniko, K.Y.: Validation of the Snow Submodel of the Biosphere–Atmosphere Transfer Scheme with Russian Snow Cover and Meteorological Observational Data, J. Climate, 10, 353–373, doi: 10.1175/1520-0442(1997)010<0353:VOTSSO>2.0.CO;2, 1997.

Yarnell, S. M., Viers, J. H., and Mount, J. F.: Ecology and Management of the Spring Snowmelt Recession, Bioscience, 60, 114-127, 10.1525/bio.2010.60.2.6, 2010.

Ye, H., Cohen, J., and Rawlins, M.: Discrimination of Solid from Liquid Precipitation over Northern Eurasia Using Surface Atmospheric Conditions, Journal of Hydrometeorology, 14, 1345-1355, 10.1175/jhm-d-12-0164.1, 2013.

Yucel, I., Onen, A., Yilmaz, K. K., and Gochis, D. J.: Calibration and evaluation of a flood forecasting sytem: Utility of numerical weather prediction model, data assimilate, and satellite-based rainfall, Journal of Hydrology, 523, 49-66, 10.1016/j.hydrol.2015.01.042, 2015.

Zängl, G.: Interaction between dynamics and cloud microphysics in orographic precipitation enhancement: A high-resolution modeling study of two North Alpine heavy-precipitation events, Monthly weather review, 135, 2817-2840, 2007.

Zanotti, F., Endrizzi, S., Bertoldi, G. and Rigon, R.: The GEOTOP snow module, Hydrolgical Processes, 18, 3667–3679. doi:10.1002/hyp.5794, 2004.

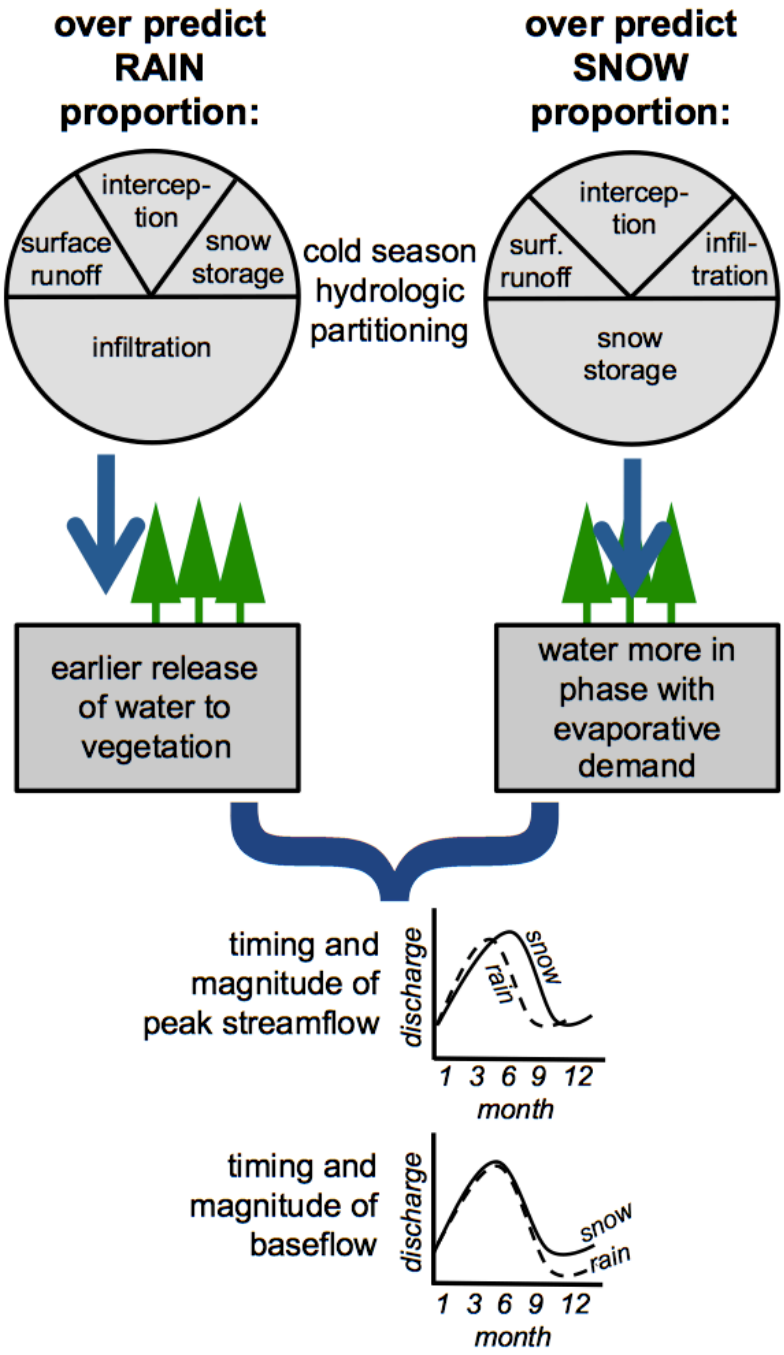

Figure 1: Precipitation phase has numerous implications for modeling the magnitude, storage, partitioning, and timing of water inputs and outputs. Potentially affecting important ecohydrological and streamflow quantities important for prediction.

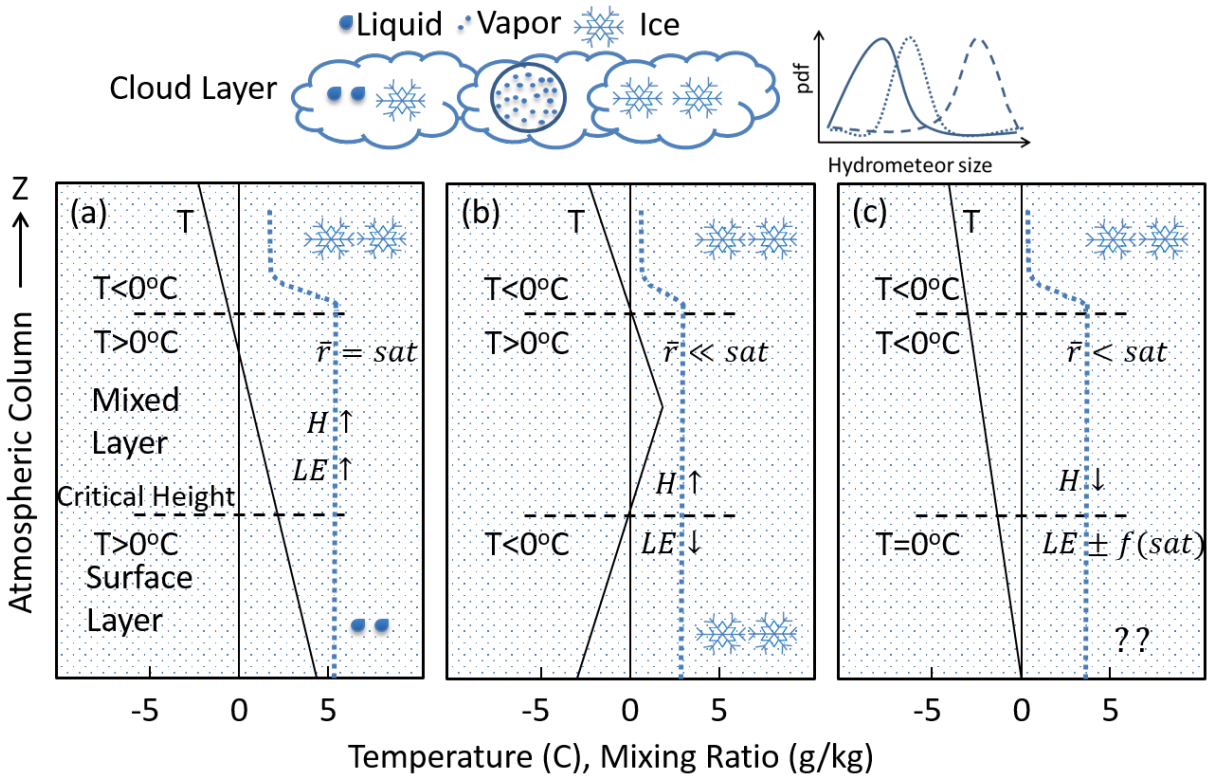

Figure 2: The phase of precipitation at the ground surface is strongly controlled by atmospheric profiles of temperature and humidity. While conditions exist that are relatively easy to predict rain (a) and snow (b), many conditions lead to complex heat exchanges that are difficult to predict with ground based observations alone (c). The blue dotted line represents the mixing ratio. H, LE, f(sat), and r are abbreviations for sensible heat, latent heat of evaporation, function of saturation and mixing ratio respectively. The arrows after H or LE indicate the energy of the hydrometeor either increasing (up) or decreasing (down) which is controlled by other atmospheric conditions.

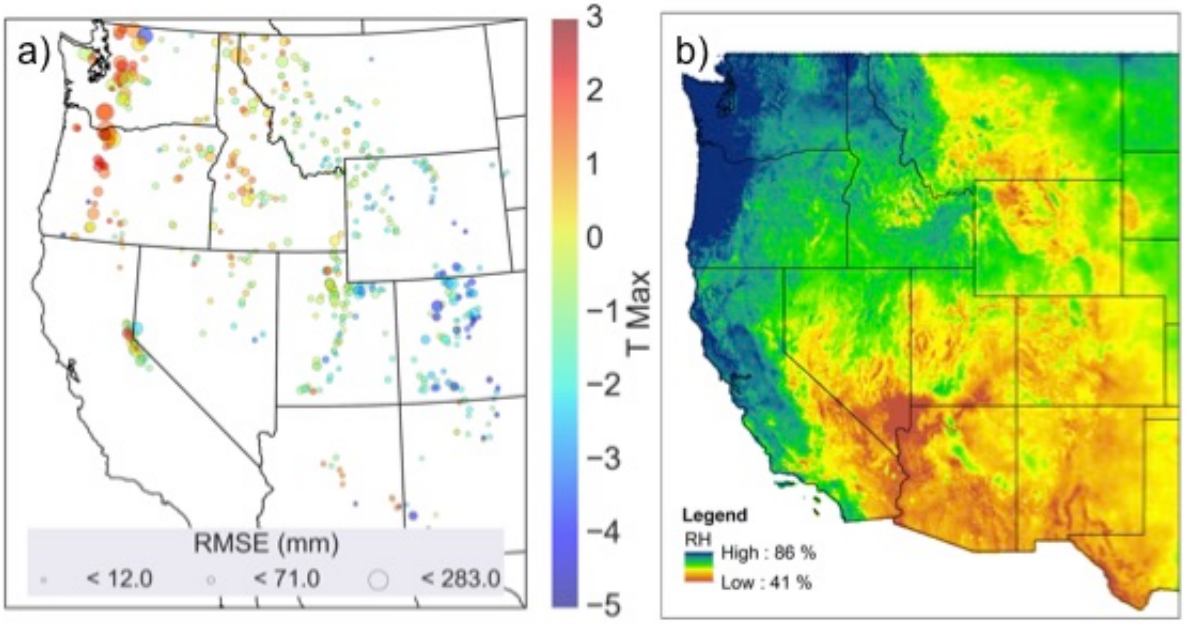

Figure 3: The optimized critical maximum daily temperature threshold that produced the lowest Root Mean Square Error (RMSE) in the prediction of snowfall at Snow Telemetry (SNOTEL) stations across the western US (adapted from Rajagopal and Harpold, 2016). b) Precipitation day relative humidity averaged over 1981-2015 based on the Gridmet dataset (Abatzoglou, 2013).

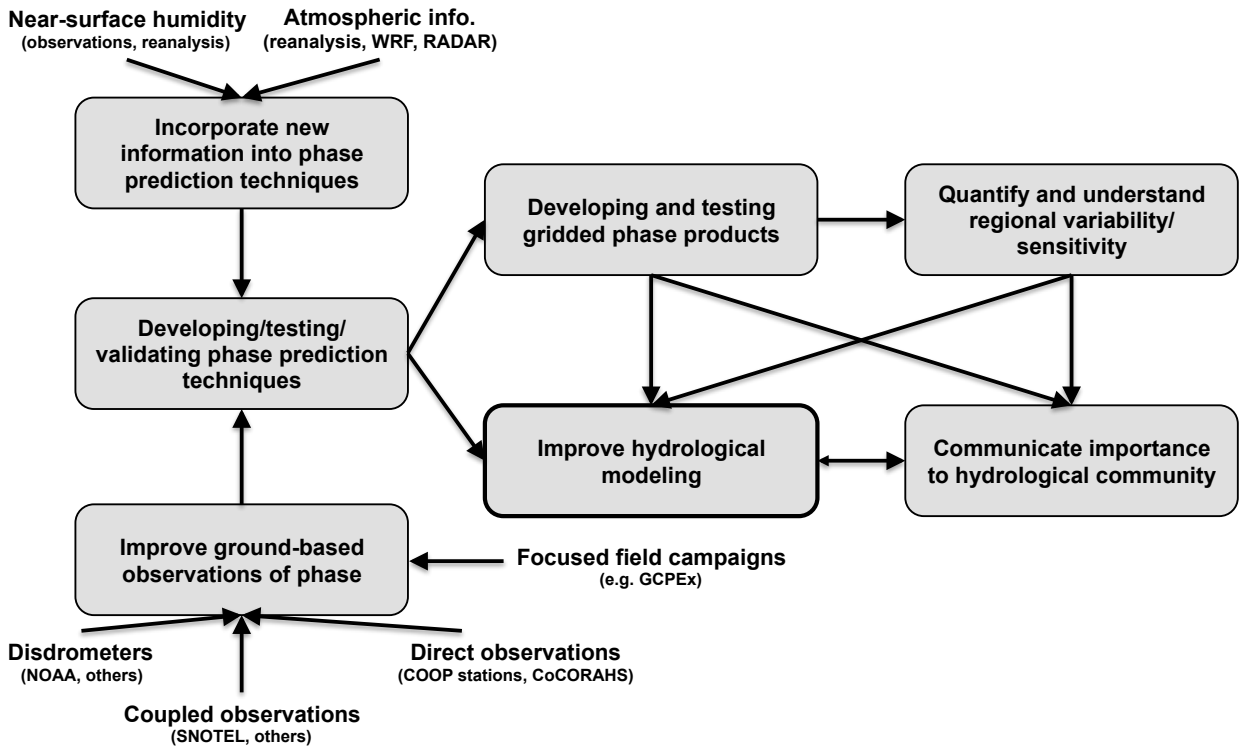

Figure 4: Conceptual representation of the research gaps and workflows needed to advance PPM and improve hydrological modeling.

Table 1. Mathematical expression for the four common temperature-based PPM to estimate snow fraction (S) or snow frequency (F) using the mean air temperature (T_a), max daily air temperature ($T_{a\text{-}max}$), and/or minimum daily air temperature ($T_{a\text{-}min}$). The variable T_{snow} is air temperature when all precipitation (P) is snow and T_{rain} is the air temperature when all air precipitation is rain.

Type	Mathematical expression for snow fraction (S) or snow frequency (F)	Reference(s)
Static threshold	$S = \begin{cases} P \; for \; T_a \leq T_{snow} \\ 0 \; for \; T_a \geq T_{snow} \end{cases}$	Motoyama, 1990
Linear transition	$S = \begin{cases} P \; for \; T_a \leq T_{snow} \\ P\left(\frac{T_{rain} - T_a}{T_{rain} - T_{snow}}\right) \; for \; T_{snow} < T_a < T_{rain} \\ 0 \; for \; T_a \geq T_{snow} \end{cases}$	McCabe and Wolock, 1998b
Minimum and maximum temperature	$S = \begin{cases} P \; for \; T_{a-max} \leq T_{snow} \\ 1 - P\left[\frac{(T_{a-max} - T_{snow})}{(T_{a-max} - T_{a-min})}\right] for \; T_{snow} < T_{a-max} < T_{rain} \\ 0 \; for \; T_{a-max} \geq T_{rain} \end{cases}$	Leavesley, 1996
Sigmoidal curve	$S = P * a\left[\tanh\left(b(T_a - c)\right) - d\right]$ $F = a\left[\tanh\left(b(T_a - c)\right) - d\right]$	Dai, 2008

Table 2. Common hydrological models and the precipitation phase prediction (PPM) technique employed. The citation referring to the original publication of the model is given.

Model	PPM technique	Citations
Discrete Models (not coupled)		
HBV	Static Threshold	Bergström, 1995
Snowmelt Runoff Model	Static Threshold	Martinec et al., 2008
SLURP	Static Threshold	Kite, 1995
UBC Watershed Model	Linear Transition	Pipes and Quick, 1977
PRMS model	Minimum & Maximum Temperature	Leavesley et al., 1996
USGS water budget	Linear transition between two mean temps	McCabe and Wolock, 1999a
SAC-SMA (SNOW-17)	Static Threshold	Anderson, 2006
DHSVM	Linear transition (double check)	Wigmosta et al., 1994
SWAT	Threshold Model	Arnold et al., 2012
RHESSys	Linear transition or input phase	Tague and Band, 2004
HSPF	Air and dew point temperature thresholds	Bicknell et al., 1997
THE ARNO MODEL	Static Threshold	Todini, 1996
HEC-1	Static Threshold	HEC-1, 1998
MIKE SHE	Static Threshold	MIKE-SHE User Manual
SWAP	Static Threshold	Gusev and Nasonova, 1998
BATS	Static Threshold	Yang et al., 1997
Utah Energy Balance	Linear Transition	Tarboton and Luce, 1996
SNOBAL/ISNOBAL	Linear Transition*	Marks et al., 2013
CRHM	Static Threshold	Fang et al., 2013
GEOTOP	Linear Transition	Zanotti et al. 2004
SNTHERM	Linear Transition	SNTHERM Online Documentation
Offline LS models		
Noah	Static Threshold	Mitchell et al., 2005
VIC	Static Threshold	VIC Documentation
CLASS	Multiple Methods+	Verseghy, 2009

* by default. Temperature-phase-density relationship explicitly specified by user.

+ A flag is specified which switches between, static threshold, linear transition.

Table 3: Remote sensing technologies useful to precipitation phase discrimination organized into ground-based, spaceborne with passive microwave, and passive with active microwave. The table describes the variables of interest, their temporal and spatial coverage, and associated references.

Technology	Variables	Spatial resolution; coverage	Temporal resolution, period of record	References
Ground-based systems				
Vertically pointing, single polarized 915-MHz Doppler wind profilers	Reflectivity, brightband height, Doppler vertical velocity	100 m vertical resolution; deployed locally in Sierra Nevada basins	Hourly, Winters 1998, 2001 - 2005	White et al., 2002; Lundquist et al., 2008
NEXRAD Dual polarized radar	Reflectivity[1], hydrometeor classification[1], melting layer[1], hybrid hydrometeor classification[1]	0.5° azimuthal by 250 m; range 460 km; Nationwide[2]	5 - 10 minutes; 2011[3] - present	Giangrande et al., 2008; Park et al., 2009; Elmore, 2011; Grazioli et al., 2015
Spaceborne systems: Passive microwave				
NOAA-15, NOAA-16, NOAA-17 Advanced Microwave Sounding Unit-A, B	Brightness temperature	48 km (AMSU-A), 16 km (AMSU-B); global coverage, with 22000 km swath	For two platforms, 6 hours revisit time; three platforms, 4 hours revisit time[4]; 1998 - present	Kongoli et al., 2003
SUOMI-NPP Advanced Technology Microwave Sounder	Brightness temperature	15 - 50 km; global coverage, with 2200 km swath	Daily; 2011 - present	Kongoli et al., 2015
GPM Core Observatory Microwave Imager	Brightness temperature	4.4 km by 7.3 km; global coverage, 904 km swath	2014 to present	Skofronick-Jackson et al., 2015
Spaceborne systems: Active microwave				
Cloud Profiling Radar (CPR)	Radar reflectivity, 2C-SNOW-PROFILE	1.4 by 1.7 km; swath 1.4 km	16 days; 2006 to present	Wood et al., 2013; Cao et al., 2014; Kulie et al., 2016;
GPM Core Observatory Dual-frequency Precipitation Radar	Radar reflectivity	5 km; global coverage, 120 - 245 km swath	2 – 4 hours; 2014 to present	Skofronick-Jackson et al., 2015

Notes:
1. Operational products available from NOAA (2016). The operational products are not ground validated, except where analyzed for specific studies.
2. The dates given here represent the first deployments. Data temporal coverage will vary by station.
3. Gaps in coverage exist, particularly in Western States.

4. Similar instruments mounted on the NASA Aqua satellite and the European EUMETSAT MetOp series. Taking into account the similar instrumentation on multiple platforms increases the temporal spatial resolution